Oneyama. 293T-CLDN cells stably expressing CLDN1 were established by the introduction of the expression plasmids encoding CLDN1 under the control of the CAG promoter of pCAG-pm3. The Huh7-derived cell line Huh7.5.1 was kindly provided by F. Chisari. The Huh7OK1 cell line efficiently propagates HCVcc as previously described (45). Huh7, Hec1B, and HEK293 cells harboring Con1- or JFH1-based HCV SGR were prepared according to the method described in a previous report (47) and maintained in DMEM containing 10% FCS and 1 mg/ml G418 (Nakalai Tesque, Kyoto, Japan).

Antibodies and drugs. Mouse monoclonal antibodies to HCV nonstructural protein 5A (NS5A) and β-actin were purchased from Austral Biologicals (San Ramon, CA) and Sigma-Aldrich, respectively. Mouse anti-ApoE antibody was purchased from Santa Cruz Biotechnology (Santa Cruz, CA). Rabbit anti-HCV core protein and NS5A were prepared as described previously (41). Rabbit anti-SR-BI antibody was purchased from Novus Biologicals (Littleton, CO). Rabbit anti-CLDN1 and -OCLN antibodies, Alexa Fluor 488 (AF488)-conjugated anti-rabbit or -mouse IgG antibodies, and AF594-conjugated anti-mouse IgG2a antibodies were purchased from Invitrogen (San Diego, CA). Mouse anti-FKBP8 antibody was described previously (44). Mouse anti-double-stranded RNA (anti-dsRNA) IgG2a (J1 and K2) antibodies were obtained from Biocenter Ltd. (Szirak, Hungary). The HCV NS3/4A protease inhibitor was purchased from Acme Bioscience (Salt Lake City, UT). Human recombinant alpha IFN (IFN-α) and cyclosporine were purchased from PBL Biomedical Laboratories (Piscataway, NJ) and Sigma-Aldrich, respectively. BODIPY 558/568 lipid probe was purchased from Invitrogen. The locked nucleic acid (LNA) targeted to miR-122, LNA-miR-122 (5′-CcAttGTcaCaCtCC-3′), and its negative control, LNA-control (5′-CcAttCTgaCcCtAC-3′) (LNAs are in capital letters, DNAs are in lowercase letters; sulfur atoms in oligonucleotide phosphorothioates are substituted for nonbridging oxygen atoms; the capital C indicates LNA methylcytosine), were purchased from Gene Design (Osaka, Japan) (15).

Preparation of viruses. pHH-JFH1-E2p7NS2mt was introduced into Huh7.5.1 cells, HCVcc in the supernatant was collected after serial passages (39), and infectious titers were determined by a focus-forming assay and expressed in focus-forming units (FFUs) (62). Mutant HCVcc was produced from Huh7.5.1 cells expressing MT miR-122 according to the method of a previous report with minor modifications (25). HCVpv, a pseudotype vesicular stomatitis virus (VSV) bearing HCV E1 and E2 glycoproteins, was prepared as previously described (61), and infectivity was assessed by luciferase expression on a Bright-Glo luciferase assay system (Promega), following a protocol provided by the manufacturer and expressed in relative light units (RLUs).

Lipofection and lentiviral gene transduction. Cells were transfected with the plasmids by using Trans IT LT-1 transfection reagent (Mirus, Madison, WI) according to the manufacturer's protocol. LNAs were introduced into cells by Lipofectamine RNAiMAX (Invitrogen). The lentiviral vectors and ViraPower lentiviral packaging mix (Invitrogen) were cotransfected into 293T cells, and the supernatants were recovered at 48 h posttransfection. The lentivirus titer was determined by a Lenti-XTM quantitative reverse transcription-PCR (qRT-PCR) titration kit (Clontech, Mountain View, CA), and the expression levels of miR-122 and AcGFP were determined at 48 h postinoculation.

Quantitative RT-PCR. HCV RNA levels were determined by the method described previously (18). Total RNA was extracted from cells by using an RNeasy minikit (Qiagen). The first-strand cDNA synthesis and qRT-PCR were performed with TaqMan EZ RT-PCR core reagents and an ABI Prism 7000 system (Applied Biosystems), respectively, according to the manufacturer's protocols. The primers for TaqMan PCR targeted to the noncoding region of HCV RNA were synthesized as previously reported (42). To determine the expression levels of miR-122, total miRNA was prepared by using the miRNeasy minikit, and miR-122 expression was determined by using fully processed miR-122-specific RT and PCR primers provided in the TaqMan microRNA assays according to the manufacturer's protocol. U6 small nuclear RNA was used as an internal control. Fluorescent signals were analyzed with the ABI Prism 7000 system.

Immunoblotting. Cells were lysed on ice in lysis buffer (20 mM Tris-HCl [pH 7.4], 135 mM NaCl, 1% Triton X-100, 10% glycerol) supplemented with a protease inhibitor mix (Nacalai Tesque). The samples were boiled in loading buffer and subjected to 5 to 20% gradient SDS-PAGE. The proteins were transferred to polyvinylidene difluoride membranes (Millipore, Bedford, MA) and reacted with the appropriate antibodies. The immune complexes were visualized with SuperSignal West Femto substrate (Pierce, Rockford, IL) and detected with an LAS-3000 image analyzer system (Fujifilm, Tokyo, Japan).

Immunofluorescence assay. Cells cultured on glass slides were fixed with 4% paraformaldehyde (PFA) in phosphate-buffered saline (PBS) at room temperature for 30 min, permeabilized for 20 min at room temperature with PBS containing 0.2% Triton, after being washed three times with PBS, and blocked with PBS containing 2% FCS for 1 h at room temperature. The cells were incubated with PBS containing appropriate primary antibodies at room temperature for 1 h, washed three times with PBS, and incubated with PBS containing AF488- or AF594-conjugated secondary antibodies at room temperature for 1 h. For lipid droplet staining, cells incubated in medium containing 20 μg/ml BODIPY for 20 min at 37°C were washed with prewarmed fresh medium and incubated for 20 min at 37°C. Cell nuclei were stained with DAPI (4′,6-diamidino-2-phenylindole). Cells were observed with a FluoView FV1000 laser scanning confocal microscope (Olympus, Tokyo, Japan).

***In vitro* transcription, RNA transfection, and colony formation.** The plasmids pSGR-Con1 and pSGR-JFH1 were linearized with ScaI and XbaI, respectively, and treated with mung bean exonuclease. The linearized DNA was transcribed *in vitro* by using a MEGAscript T7 kit (Applied Biosystems) according to the manufacturer's protocol. The *in vitro*-transcribed RNA (10 μg) was electroporated into Hec1B and HEK293 cells at 10^7 cells/0.4 ml under conditions of 190 V and 975 μF using a Gene Pulser apparatus (Bio-Rad, Hercules, CA) and plated on DMEM containing 10% FCS. The medium was replaced with fresh DMEM containing 10% FCS and 1 mg/ml G418 at 24 h posttransfection. The remaining colonies were cloned by using a cloning ring (Asahi Glass, Tokyo, Japan) or fixed with 4% PFA and stained with crystal violet at 4 weeks postelectroporation.

Electron microscopy and correlative FM-EM analysis. Cells were cultured on a Cell Desk polystyrene coverslip (Sumitomo Bakelite) and were fixed with 2% formaldehyde and 2.5% glutaraldehyde in 0.1 M cacodylate buffer (pH 7.4) containing 7% sucrose. Cells were postfixed for 1 h with 1% osmium tetroxide and 0.5% potassium ferrocyanide in 0.1 M cacodylate buffer (pH 7.4), dehydrated in graded series of ethanol, and embedded in Epon812 (TAAB). Ultrathin (80-nm) sections were stained with saturated uranyl acetate and lead citrate solution. Electron micrographs were obtained with a JEM-1011 transmission electron microscope (JEOL). Correlative fluorescence microscopy (FM)-electron microscopy (EM) allows individual cells to be examined both in an overview with FM and in a detailed subcellular-structure view with EM (51). The NS5A was stained and observed in the Hec1B-derived Con1 SGR cells by the correlative FM-EM method as described previously (44).

Intracellular infectivity. Intracellular viral titers were determined according to a method previously reported (20). Briefly, cells were extensively washed with PBS, scraped, and centrifuged for 5 min at 1,000 × *g*. Cell pellets were resuspended in 500 μl of DMEM containing 10% FCS and subjected to three cycles of freezing and thawing using liquid nitrogen and a thermo block set to 37°C. Cell lysates were centrifuged at 10,000 × *g* for 10 min at 4°C to remove cell debris. Cell-associated infectivity was determined by a focus-forming assay.

Statistical analysis. The data for statistical analyses are averages of three independent experiments. Results were expressed as means ± standard deviations. The significance of differences in the means was determined by Student's *t* test.

Microarray data accession number. Access to data concerning this study may be found under GEO experiment accession number GSE32886.

RESULTS

Nonhepatic cell lines susceptible to HCVcc by expression of miR-122. Human CD81 (hCD81), SR-B1, CLDN1, and OCLN are crucial for HCV entry (16, 48, 49, 56). First, we examined the expression of these receptor candidates in nonhepatic cell lines by using the web-based NextBio search engine (Cupertino, CA). Multidimensional scaling was used to visualize the differences in expression patterns of molecules of various tissues, cells, and cell lines from those of hepatic cell lines and primary hepatocytes. We selected nine nonhepatic cell lines as possibly being susceptible to HCVcc infection: NCI-H-2030 (lung), Caki-2 (kidney), 769-P (bladder), A-427 (lung), SK-OV3 (ovary), SW780 (bladder), SW620 (colon), RERF-LC-AI (lung), and Hec1B (uterus) (Fig. 2). In addition, three nonhepatic cell lines previously reported to be susceptible to replication of HCV RNA—that is, SK-PN-DW (neuron), MC-IXC (neuron), and 293T-CLDN (kidney)—were included in this study (8, 17). The expression of each receptor molecule in these 12 nonhepatic cell lines was confirmed by fluorescence-activated cell sorter (FACS) analysis and immunoblotting (Fig. 3A and B). To examine the expression of the functional receptors for HCV entry in these cell lines, we inoculated HCVpv into the cells. Ten of the cell lines (A-427 and SW780 being the exceptions) exhibited various degrees of susceptibility to HCVpv infection (Fig. 3C). Therefore, we examined the possibility of propagation of HCVcc by the expression of miR-122 in these 10 cell lines.

To introduce miR-122 in the cell lines, we employed a lentiviral vector encoding pri-miR-122, an unprocessed miR-122. To confirm the maturation of pri-miR-122 to form functional RNA-induced silencing complexes (RISCs), suppression of the translation of the target mRNA was determined by a dual reporter assay. Translation of a firefly luciferase mRNA containing the sequences complementary to miR-122 in the 3′ UTR was suppressed by infection with the lentivirus encoding pri-miR-122 but not by infection with a control virus (data not shown), suggesting that the pri-miR-122 is processed into a functionally mature miR-122. By using this lentiviral vector, high levels of miR-122 expression were achieved in the 10 cell lines, comparable to the endogenous expression level of miR-122 in Huh7 cells (Fig. 4A).

To examine the effect of the exogenous expression of miR-122 on HCV replication, the nonhepatic cell lines expressing miR-122 were infected with HCVcc at a multiplicity of infection (MOI) of 1, and intracellular viral RNA was determined (Fig. 4B). The expression of miR-122 significantly increased the amount of the HCV genome in Hec1B, 293T-CLDN, MC-IXC, and RERF-LC-AI cells as well as Huh7 cells and slightly increased it in SK-OV3 and NCI-H-2030 cells. Although the levels of viral RNA in SW620, Caki-2, and SK-PN-DW cells upon expression of miR-122 were higher than those in control cells, no increase of viral RNA was observed. No effect of the expression of miR-122 was observed in 769-P cells. Interestingly, naïve Hec1B cells exhibited a delayed increase in viral RNA from 24 to 48 h postinfection, in contrast to the gradual decrease of viral RNA in other cell lines. Replication of HCV RNA in both naïve and miR-122-expressing Hec1B cells was inhibited by treatment with an inhibitor for HCV protease but not by treatment with IFN-α, due to the lack of an IFN receptor (11), whereas treatments with either IFN-α or the protease inhibitor suppressed the replication of HCV in the other cell lines expressing miR-122 (Fig. 4C). These results indicate that exogenous miR-122 expression enhances the replication of HCV even in nonhepatic cells. Hec1B cells exhibit a delayed replication of HCV, and HCV replication was enhanced by the exogenous expression of miR-122. Therefore, in this study we used Hec1B cells to investigate the biological significance of miR-122 on the replication of HCVcc in nonhepatic cells.

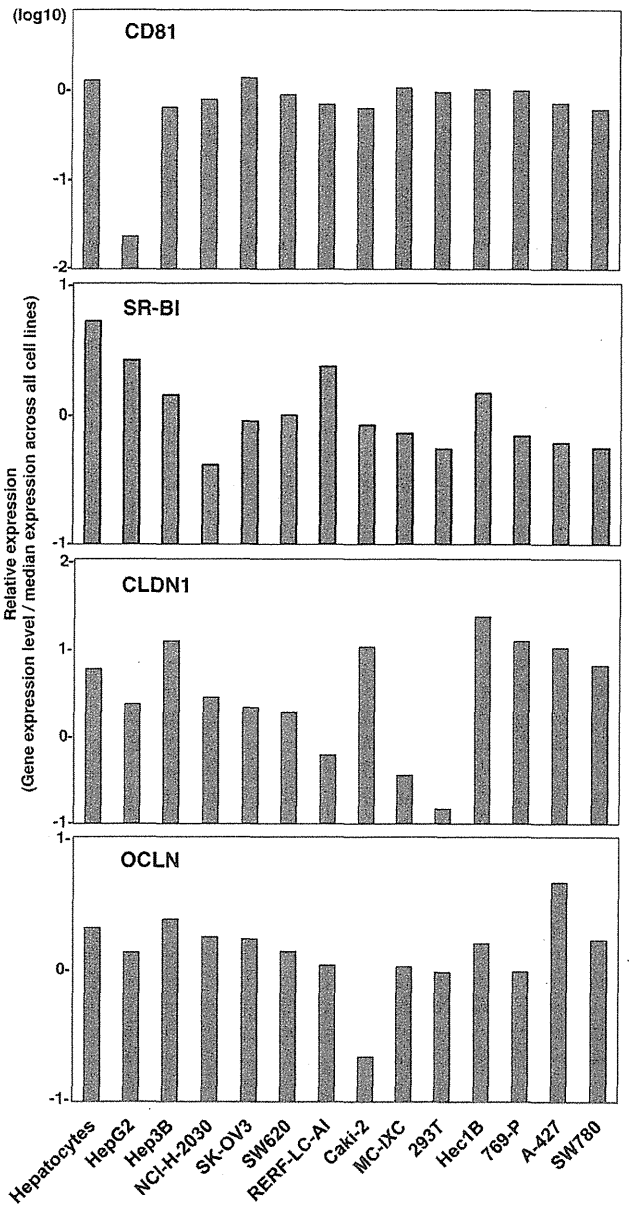

FIG 2 Receptor expression profiling in nonhepatic cells. Relative expression levels of CD81, SR-BI, CLDN1, and OCLN in primary hepatocytes, hepatic cell lines HepG2 and Hep3B, and nonhepatic cells were determined by using the NextBio Body Atlas. Expression levels were standardized by the median expression across all cell lines.

Expression of miR-122 is essential for enhancing HCV replication in Hec1B cells. To confirm the specificity of HCV replication in Hec1B cells, HCVcc was preincubated with an anti-HCV E2 monoclonal antibody, AP-33, or Hec1B/miR-122 and Hec1B/

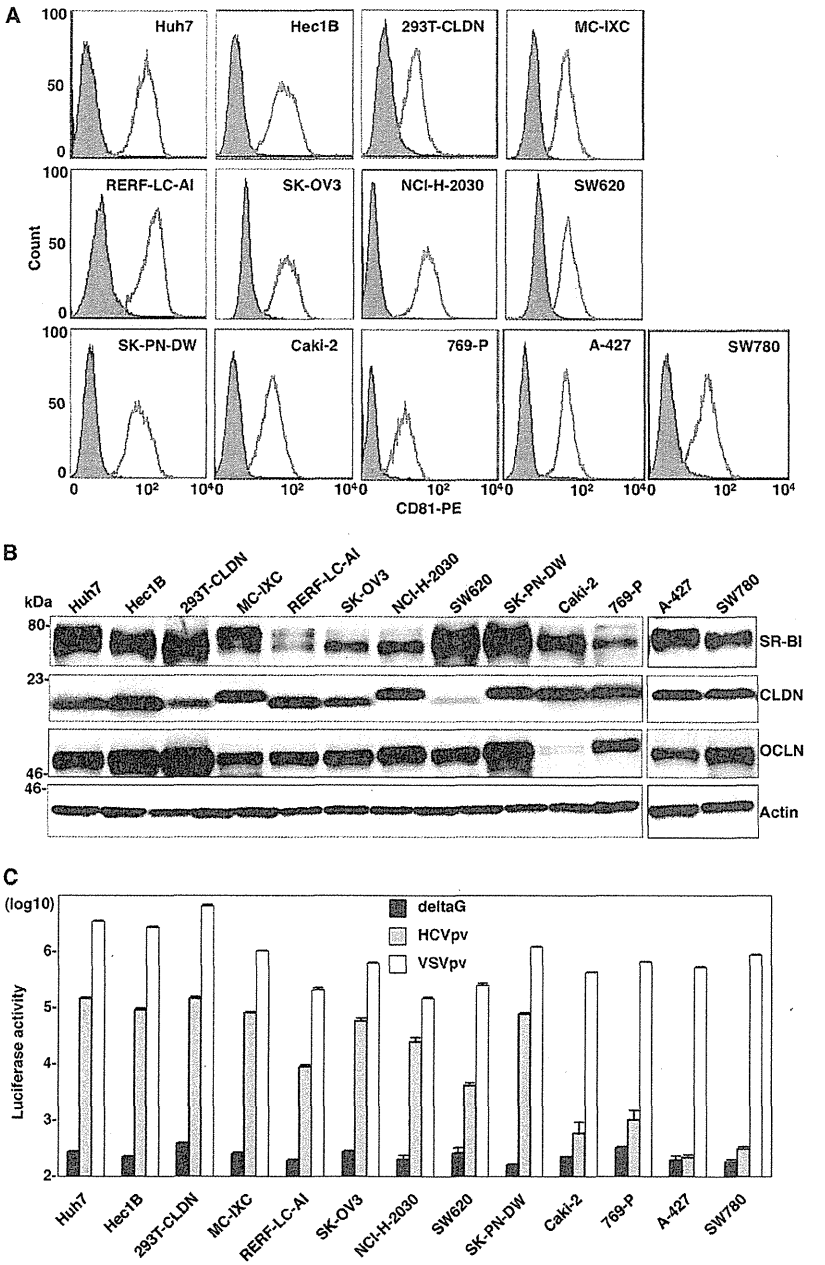

FIG 3 Expression of functional HCV receptor candidates in nonhepatic cells. (A) Expression of hCD81 in nonhepatic cells was determined by flow cytometry. PE, phycoerythrin. (B) Expression levels of SR-B1, CLDN, and OCLN in the nonhepatic cells were determined by immunoblotting. (C) The nonhepatic cell lines were inoculated with pseudotype VSVs bearing no envelope protein (deltaG), HCV envelope proteins of genotype 1b Con1 strain (HCVpv), or VSV G protein (VSVpv), and luciferase expression was determined at 24 h postinfection.

Cont cells were pretreated with anti-hCD81 monoclonal antibody. Replication of HCV RNA was determined upon infection with HCVcc. The antibody treatment significantly inhibited HCV replication in the Hec1B cell line, indicating that HCVcc internalizes into Hec1B cells through a specific interaction between hCD81 and E2 (Fig. 5). Next, we determined the dose dependence of miR-122 expression on the enhancement of HCV replication in Hec1B cells. Huh7.5.1 and Hec1B cells transduced with the lentiviral vector encoding pri-miR-122 were infected with HCVcc at an MOI of 1, and intracellular miR-122 and viral RNA were determined. Expression of miR-122 was increased in Hec1B cells in a dose-dependent manner of the lentivirus, whereas no increase was observed in Huh7.5.1 cells, probably due to the high level of endogenous expression of miR-122 (Fig. 6A, left). HCV RNA replication in Huh7.5.1 and Hec1B cells was correlated with miR-122 expression (Fig. 6A, right), suggesting a close correlation between miR-122 expression and HCV replication.

Next, we examined the expression of viral proteins in Hec1B/

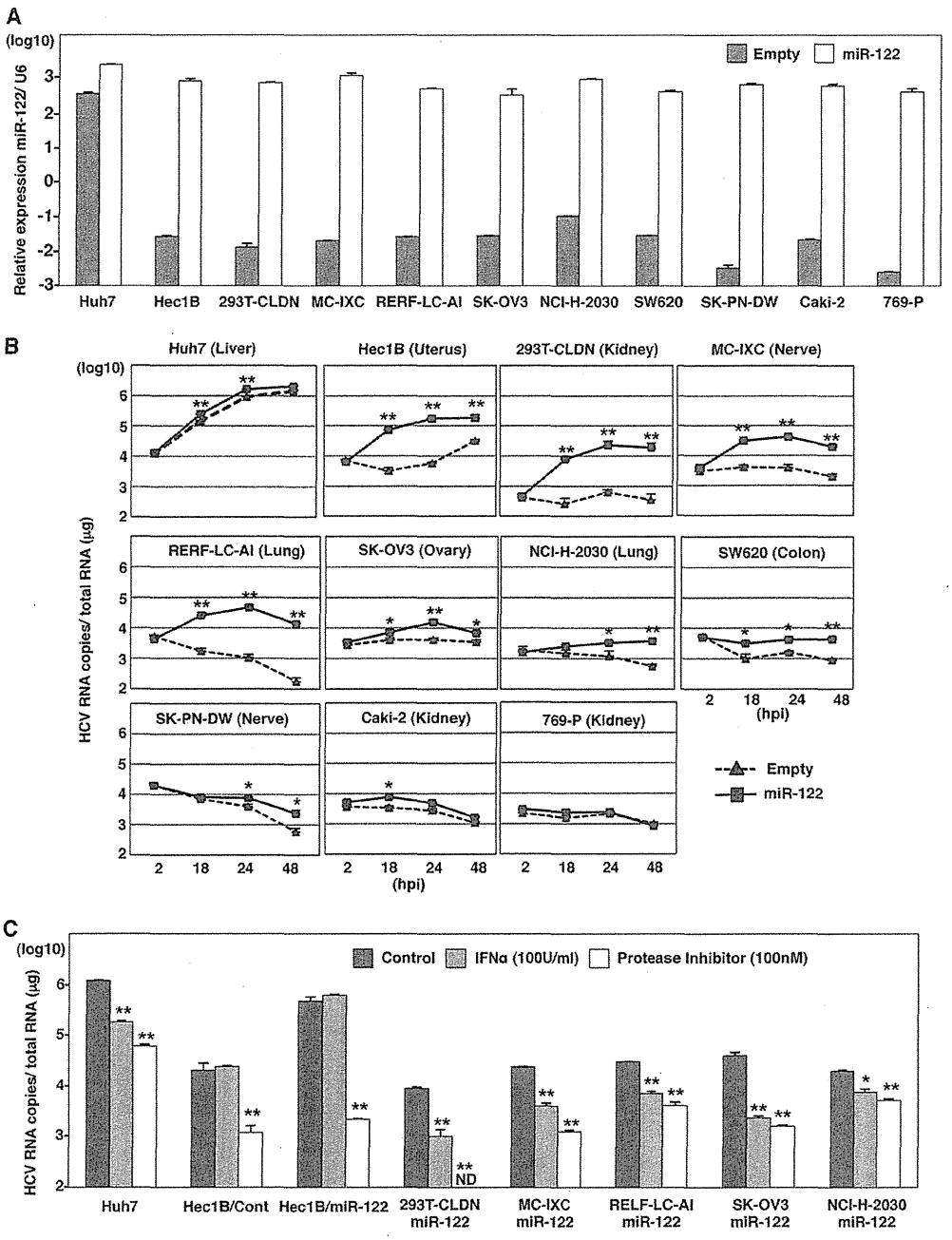

FIG 4 Nonhepatic cell lines susceptible to HCVcc by the expression of miR-122. (A) Exogenous miR-122 was expressed in Huh7, Hec1B, 293T-CLDN, MC-IXC, RERF-LC-AI, SK-OV3, NCI-H-2030, SW620, Caki-2, SK-PN-DW, and 769-P cells by lentiviral vector. Total RNA was extracted from the cells and subjected to qRT-PCR analysis. U6 was used as an internal control. Gray and white bars, endogenous and exogenous levels of miR-122, respectively. (B) HCVcc was inoculated into Huh7 and nonhepatic cell lines expressing (solid lines) or not expressing (dashed lines) exogenous miR-122 at an MOI of 1. Intracellular HCV RNA levels were determined by qRT-PCR at 2, 18, 24, and 48 h postinfection (hpi). (C) Cells were inoculated with HCVcc and simultaneously treated with either 100 U IFN-α or 100 nM HCV protease inhibitor or not treated (control), and intracellular HCV RNA levels were determined by qRT-PCR at 36 h postinfection. Asterisks indicate significant differences (*, $P < 0.05$; **, $P < 0.01$) versus the results for control cells.

miR-122 cells upon infection with HCVcc by immunoblotting and fluorescence microscopic analyses (Fig. 6B). Expression of NS5A protein was increased in Hec1B/miR-122 cells in an MOI-dependent manner. Expression of NS5A in Hec1B/Cont cells infected with HCVcc at an MOI of 3 was significantly lower than that in Hec1B/miR-122 cells infected with HCVcc at an MOI of 0.5. HCV core and NS proteins were shown to localize mainly on the lipid droplets and cytoplasmic face of the endoplasmic reticulum (ER) in Huh7 and Hep3B/miR-122 cells infected with HCVcc (29, 40). Immunofluorescence analyses revealed that HCV core and NS5A proteins were colocalized with lipid droplets and calnexin, an ER marker, in Hec1B cells infected with HCVcc (Fig. 7).

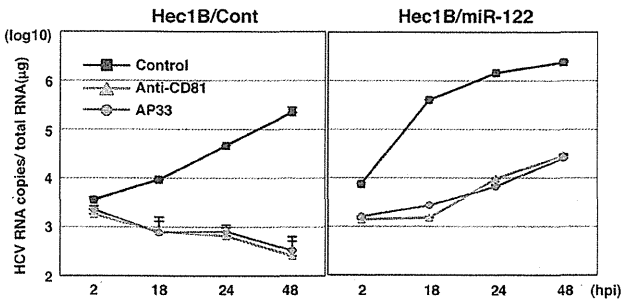

FIG 5 Neutralization of HCVcc infection in Hec1B cells by specific antibodies. HCVcc was preincubated with anti-E2 antibody (AP-33) and inoculated into Hec1B/Cont and Hec1B-miR-122 cells. Cells were preincubated with anti-human CD81 antibody and inoculated with HCVcc. Intracellular HCV RNA levels at 2, 18, 24, and 48 h postinfection were determined by qRT-PCR.

To further confirm the specificity of the enhancement of HCV replication by the expression of miR-122, Huh7, Hec1B/miR-122, and Hec1B/Cont cells were treated with LNAs that were either specific to miR-122 (LNA-miR-122) or nonspecific (LNA-control) at 6 h before infection with HCVcc. Although the treatment with LNA-miR-122 inhibited the enhancement of viral RNA replication in Huh7 and Hec1B/miR-122 cells in a dose-dependent manner, no inhibition of viral replication was observed in Hec1B/Cont cells (Fig. 6C). These results suggest that Hec1B cells permit HCV replication in a miR-122-independent manner and exogenous expression of miR-122 enhances viral replication.

Specific interaction between miR-122 and the 5′ UTR of HCV is required for HCV replication. To determine the effect of the specific interaction between miR-122 and the 5′ UTR of the HCV genome on the enhancement of RNA replication, we generated MT pri-miR-122 carrying a substitution of uridine to adenosine in the seed domain and an additional complementary substitution of adenosine to uridine to stabilize the loop structure of pri-miR-122 (Fig. 8A). A high expression level of MT miR-122, comparable to that of WT miR-122, was introduced into Hec1B cells by infection with lentiviral vectors (Fig. 8B). To determine the specificity of miR-122 on the replication of HCV, Hec1B cells expressing either WT or MT miR-122 were inoculated with HCVcc at an MOI of 1. Enhancement of HCV replication was observed in Hec1B cells by the expression of WT but not that of MT miR-122, suggesting that the sequence specificity of miR-122 with the 5′ UTR of HCV is crucial for the efficient replication of HCV (Fig. 8C). To further confirm the effect of the specificity of interaction between miR-122 and the binding sites in the 5′ UTR of HCV on the enhancement of HCV replication, we generated two mutant viruses, HCVcc-M1 and HCVcc-M2, carrying complementary substitutions in the miR-122-binding site 1 alone and in both sites 1 and 2 in the 5′ UTR of HCV, respectively (Fig. 8D). Recently, Jangra et al. demonstrated that the propagation of a mutant HCVcc bearing mutations in sites 1 and 2 in the 5′ UTR was rescued by the expression of MT miR-122 in Huh7.5 cells (25). We confirmed that the propagation of HCVcc-M1 and HCVcc-M2 in Huh7.5.1 cells was rescued by the expression of MT miR-122 but not of WT miR-122, although the recovery of infectious titers of HCVcc-M2 was significantly lower than the recovery of infectious titers of HCVcc-M1 (Fig. 8E). Next, to examine the interaction between miR-122 and the HCV genome in Hec1B cells, we inoculated HCVcc or mutant viruses into Hec1B cells expressing either or both WT and MT miR-122 and determined the replication of HCV RNA by qRT-PCR (Fig. 8F). Expression of WT and MT miR-122 in Hec1B cells permits replication of HCVcc and HCVcc-M2, respectively, although the enhancing effects differed. On the other hand, the expression of both WT and MT miR-122 is required for the replication of HCVcc-M1, because MT and WT miR-122 bind to sites 1 and 2 in the 5′ UTR of this virus, respectively. Interestingly, a low level of HCVcc-M1 replication was also observed in Hec1B cells expressing either WT or MT miR-122, in contrast to the requirement of the corresponding miR-122 for the replication of HCVcc and HCVcc-M2. These results suggest that the specific interaction between miR-122 and the 5′ UTR of HCV is crucial for the replication of HCV.

Viral particle formation in hepatic and nonhepatic cells. These data suggest that miR-122 expression facilitates replication of HCV RNA in nonhepatic cells. Recently, we have shown that expression of miR-122 facilitates infectious particle formation of HCVcc in a hepatoma cell line, Hep3B (29). To examine the effect of miR-122 expression on particle formation in nonhepatic cells, intracellular and extracellular viral RNA levels in cells infected with HCVcc were determined. Intracellular RNA replication in the hepatic cell lines, including Huh7.5.1 and Hep3B/miR-122, was increased up to 72 h postinfection with HCVcc, whereas in nonhepatic cell lines, including 293T-CLDN/miR-122 and Hec1B/miR-122, such replication was comparable to that in the hepatic cell lines until 24 h postinfection but reached a limit at this point (Fig. 9A). In spite of no clear increase of intracellular HCV RNA in Hep3B/Cont cells upon infection with HCVcc (Fig. 9A), subtle but substantial production of infectious particles was detected in the culture supernatants at 72 h postinfection, in contrast to no production of infectious particles in those of the nonhepatic cell lines (Fig. 9B). Furthermore, no focus formation was observed in Hec1B/miR-122 cells upon infection with HCVcc, in contrast to the many foci in Huh7.5.1 cells (Fig. 9C), and no infectivity was detected even in the lysates of Hec1B/miR-122 cells infected with HCVcc (Fig. 9D). These results suggest that not only the replication efficiency of viral RNA but also other factors are involved in the assembly of HCV and that the viral assembly process is impaired in Hec1B/miR-122 cells infected with HCVcc, in spite of the efficient replication of HCV RNA.

It was previously shown that lipid droplets, diacylglycerol *O*-acyltransferase 1 (DGAT1), and apolipoproteins B and E play an important role in the assembly of HCV particles (10, 22, 40). To understand the molecular mechanisms underlying the low efficiency of infectious particle formation in nonhepatic cells, we first examined the subcellular localization of lipid droplets and HCV core protein in Hec1B/miR-122 cells infected with HCVcc. Although the core protein was detected around the lipid droplets, as seen in Huh7.5.1 cells, only a small amount of lipid droplets was detected in Hec1B/miR-122 cells infected with HCVcc compared with the amount detected in Huh7.5.1 cells (Fig. 9E), suggesting that the low level of lipid droplet formation is involved in the impairment of infectious particle formation in nonhepatic cells.

Next we examined the expression patterns of molecules involved in lipid metabolism by using cDNA microarray and qPCR analyses. Although expression levels of low-density lipoprotein receptor (LDLR), sterol regulatory element-binding protein 1c (SREBP1c), SREBP2, and DGAT1 in nonhepatic Hec1B and 293T cells were comparable to those in hepatic Huh7 and Hep3B cells, those of VLDL-associated proteins, including ApoE, ApoB, and

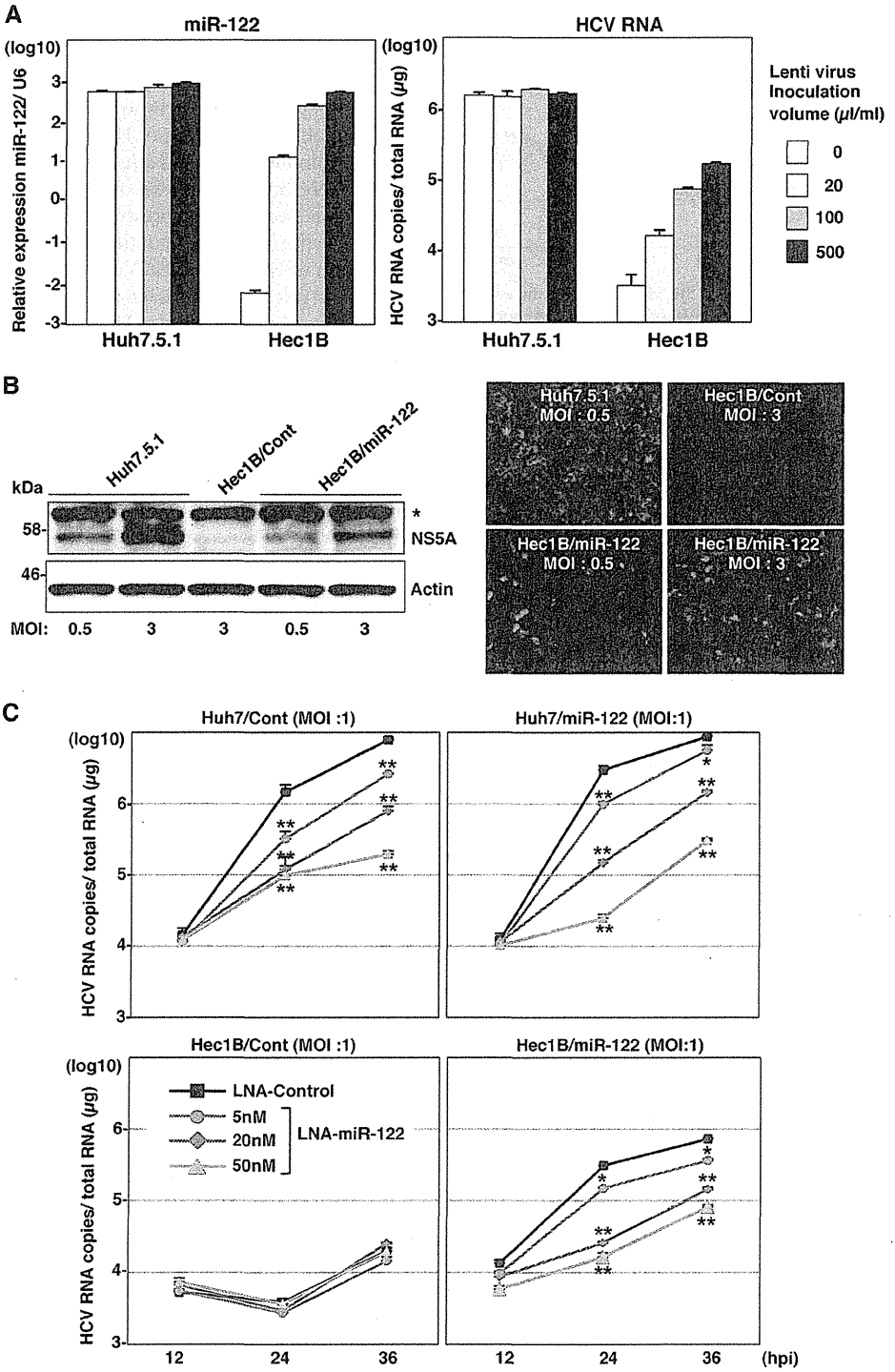

FIG 6 Expression of miR-122 is essential for the enhancement of HCV replication in the Hec1B cells. (A) Huh7.5.1 and Hec1B cells were transduced with lentiviral vectors expressing miR-122 in a dose-dependent manner and infected with HCVcc at an MOI of 1. Intracellular miR-122 and HCV RNA were determined at 24 h postinfection by qRT-PCR. (B) Huh7.5.1 and Hec1B/miR-122 cells were infected with HCVcc at an MOI of 0.5 or 3 and subjected to immunoblotting and immunofluorescence analyses using anti-NS5A antibodies at 48 h postinfection. The asterisk indicates nonspecific bands. (C) LNAs specific to miR-122 at a final concentration of 5 nM, 20 nM, or 50 nM and control (LNA alone at 50 nM) were introduced into Huh7/Cont, Huh7/miR-122, Hec1B/miR-122, and Hec1B/Cont cells by using Lipofectamine RNAiMAX transfection reagent and infected with HCVcc at an MOI of 1 at 6 h posttransfection. Intracellular HCV RNA levels were determined by qRT-PCR at 12, 24, and 36 h postinfection. Asterisks indicate significant differences (*, $P < 0.05$; **, $P < 0.01$) versus the results for control cells.

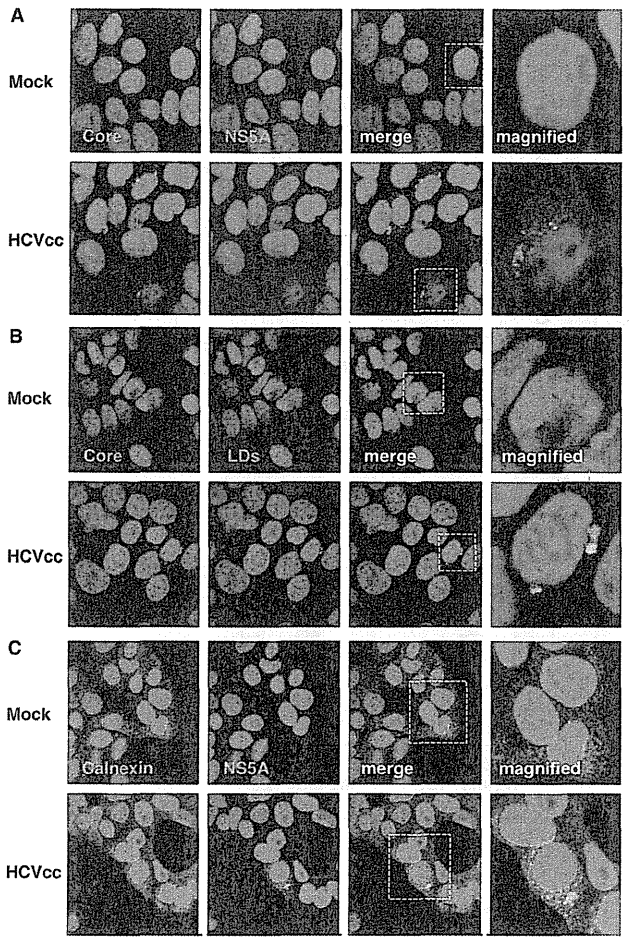

FIG 7 Subcellular localization of core and NS5A proteins in Hec1B/miR-122 cells infected with HCVcc. Hec1B/miR-122 cells infected with or without HCVcc at an MOI of 1 were fixed with 4% PFA at 48 h postinfection and stained with appropriate antibodies to core and NS5A proteins (A), core protein and lipid droplets (B), and NS5A and calnexin (C). The boxes in the merged images were magnified, and the images are displayed on the right.

MTTP, in nonhepatic cells were significantly lower than those in hepatic cells (Fig. 10). Collectively, these results suggest that intracellular functional lipid metabolism, including the biosynthesis of lipid droplets and the production of VLDL, participates in the assembly of HCV.

Establishment of HCV replicon in Hec1B/miR-122 cells. It was previously shown by using RNA replicon cells based on the JFH1 strain that expression of miR-122 enhanced the translation of HCV RNA in HEK293 cells and MEFs (8, 35). We tried to establish HCV replicon cells based on genotype 1b Con1 and genotype 2a JFH1 strains in Hec1B/miR-122 and HEK293 cells stably expressing miR-122 (HEK293/miR-122). To examine the colony formation efficiency of the HCV RNAs of the Con1 and JFH1 strains, SGR RNA was electroporated into the cell lines and selected by G418 for 3 weeks. Expression of miR-122 in Hec1B cells significantly enhanced the colony formation of SGR of the Con1 strain (Fig. 11A), suggesting that the expression of miR-122 in Hec1B cells supports the efficient replication of SGR. HCV replication in 20 replicon clones established by the transfection with SGR RNA of the Con1 strain in Hec1B/miR-122 cells was examined by qRT-PCR and immunoblotting. All clones contained high levels of HCV RNA (3×10^6 to 5×10^7 copies per μg of total RNA) (Fig. 11B), and expression of NS5A was well correlated with the levels of HCV RNA in the clones (Fig. 11C). Two replicon clones (clones 2 and 10) in Hec1B/miR-122 cells exhibiting high levels of RNA replication and NS5A expression further confirmed the high level of expression of NS5A by immunofluorescent microscopy (Fig. 11D). These results suggest that expression of miR-122 facilitates the efficient replication of SGR of at least two HCV genotypes in Hec1B cells.

Our previous reports showed that HCV NS proteins were colocalized with dsRNA and cochaperone molecules, FK506-binding protein 8 (FKBP8), in dot-like structures on the ER membrane of Huh7 replicon cells (59). Colocalization of NS5A with dsRNA or FKBP8 was observed in the dot-like structures in not only Huh7 SGR cells but also Hec1B/miR-122 SGR cells (Fig. 12A), suggesting that the dot-like structure required for efficient viral replication is also generated in Hec1B/miR-122 replicon cells. It has been shown that HCV replication induces the formation of convoluted membranous structures, called membranous webs, in Huh7 cells (13, 45). FM-EM techniques revealed the localization of NS5A on the convoluted structures in Hec1B/miR-122 replicon cells (Fig. 12B). These results suggest that the replication complex required for viral replication was also generated in the Hec1B/miR-122 replicon cells, as was seen in the Huh7 replicon cells.

miR-122 is a crucial determinant of HCVcc propagation. It has been shown that the infectivity of HCVcc in cured cells, established when IFN treatment induces the elimination of the viral genome from the Huh7 replicon cells harboring an HCV RNA, is significantly higher than that in parental Huh7 cells (2, 66). Therefore, we tried to establish Hec1B-based cured cells from the Con1 SGR clones harboring a high copy number of HCV RNA. Treatment with cyclosporine and the protease inhibitor of HCV suppressed NS5A expression in Hec1B/miR-122 SGR clone 2 in a dose-dependent manner (Fig. 13A), whereas no reduction was observed by the IFN treatment due to a lack of an IFN receptor, as shown in Fig. 4C. It was reported that monotherapy by the HCV protease inhibitor induces the emergence of resistant breakthrough viruses (34, 55). Therefore, we treated five Hec1B/miR-122 SGR clones (clones 2, 5, 10, 14, and 16) with 1 μg/ml cyclosporine and 100 nM protease inhibitor for HCV. Viral RNA was determined by qRT-PCR every 5 days posttreatment. Elimination of viral RNA was achieved in four clones (clones 2, 5, 10, and 14) within 20 days posttreatment (Fig. 13B). Replication of HCV RNA in the cured cells infected with HCVcc at an MOI of 0.5 was 2- to 30-fold higher than that in parental cells at 24 h postinfection (Fig. 13C). In addition, replication of HCV RNA in cured clone 2 infected with HCVcc at an MOI of 0.1 was comparable to that in Huh7.5.1 cells until 24 h postinfection (Fig. 13D). Expression of NS5A was significantly increased in cured clone 2 compared to that in the parental Hec1B/miR-122 cells (Fig. 13E and F). It was previously shown that the increased permissiveness of Huh7-derived cured cells, Huh7.5 cells, is attributable to a mutation in the RIG-I gene (58). To examine the innate immune response in the parental and cured Hec1B/miR-122 cells, induction of IFN-stimulated gene 15 (ISG15) was determined upon stimulation with IFN-α or VSV. Although induction of ISG15 was not observed in either parental or cured cells upon stimulation with IFN-α due to a lack of an IFN receptor (11) (Fig. 14A), it was

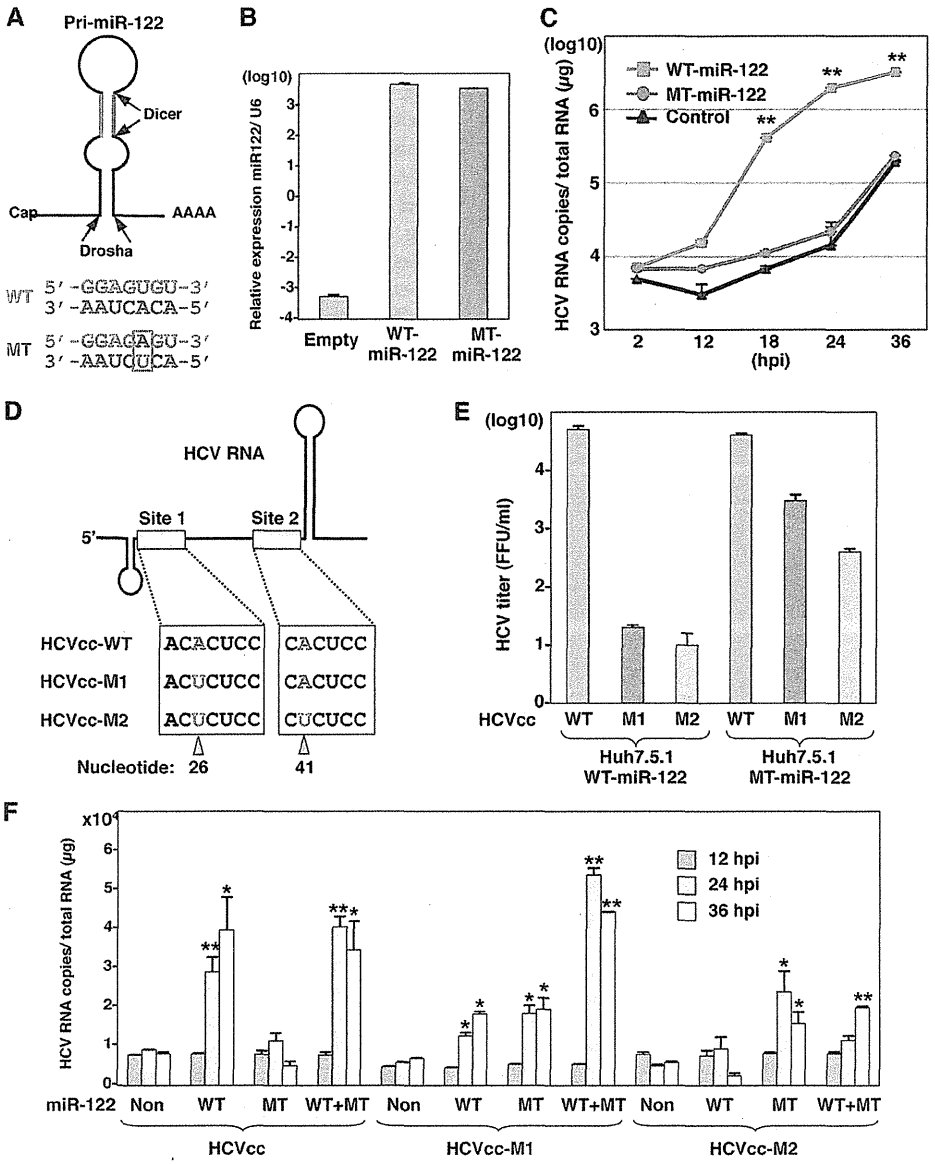

FIG 8 Specific interaction between miR-122 and the 5′ UTR of HCV is required for HCV replication. (A) Structures of pri-miR-122 and the nucleotide sequences of WT and MT miR-122, which has a substitution of uridine to adenosine in the seed domain and an additional complementary substitution of adenosine to uridine for stable expression. (B) WT or MT miR-122 was introduced into Hec1B cells by a lentiviral vector, and miR-122 expression levels were determined by qRT-PCR. (C) HCVcc was inoculated into Hec1B cells expressing either WT or MT miR-122 and control cells at an MOI of 1, and the intracellular HCV RNA levels were determined by qRT-PCR. (D) Diagram of mutant viruses HCVcc-M1 and HCVcc-M2 carrying complementary substitutions in the miR-122-binding site 1 alone and both sites 1 and 2 in the 5′ UTR of HCV, respectively. (E) Viral RNA of HCVcc, HCVcc-M1, or HCVcc-M2 was electroporated into Huh7.5.1 cells expressing either WT or MT miR-122, and infectious titers of the viruses recovered in the culture supernatants at 72 h postinfection of the second passage were determined by a focus-forming assay in cells expressing either WT or MT miR-122. Red, blue, and green bars, infectious titers of HCVcc, HCVcc-M1, and HCV-M2, respectively. (F) HCVcc, HCVcc-M1, or HCV-M2 was inoculated into Hec1B cells expressing either or both WT and MT miR-122 at an MOI of 0.5, and intracellular HCV RNA levels were determined at 12, 24, and 36 h postinfection by qRT-PCR. Asterisks indicate significant differences (*, $P < 0.05$; **, $P < 0.01$) versus the results for control cells.

detected in both cells infected with VSV (Fig. 14B). Therefore, other mechanisms should be involved in the enhancement of permissiveness of Hec1B-derived cured cells. Ehrhardt et al. showed that the expression levels of miR-122 in Huh7-derived cured cells, including Huh7.5, Huh7.5.1, and Huh7-Lunet cells, are significantly higher than those in parental Huh7 cells (14). In addition, our recent study indicated that levels of expression of miR-122 in the cured Huh7 and Hep3B/miR-122 cells were higher than those in parental cells (29). Levels of expression of miR-122 in the Hec1B-based cured cell clones are also higher than those in parental Hec1B/miR-122 cells (Fig. 13G). These results suggest that a high level of miR-122 expression is a crucial determinant of high susceptibility to HCVcc propagation in the cured cells.

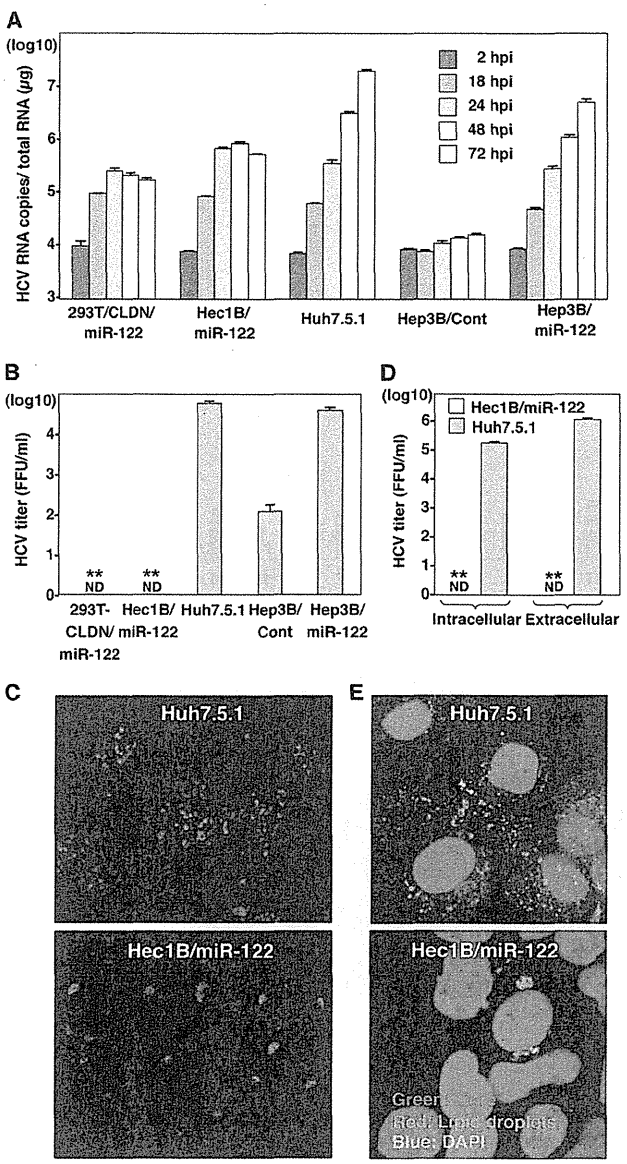

FIG 9 Viral particle formation in hepatic and nonhepatic cells. (A) HCVcc was inoculated into 293T-CLDN/miR-122, Hec1B/miR-122, Hep3B/Cont, and Hep3B/miR-122 cells at an MOI of 1 and into Huh7.5.1 cells at an MOI of 0.1. HCV RNA levels (copies/μg) in cells at 2, 18, 24, 48, and 72 h postinfection were determined by qRT-PCR. (B) HCVcc was inoculated into 293T-CLDN/miR-122, Hec1B/miR-122, Hep3B/Cont, and Hep3B/miR-122 cells at an MOI of 1 or into Huh7.5.1 cells at an MOI of 0.1, and infectious titers in the culture supernatants were determined at 72 h postinfection by a focus-forming assay in Huh7.5.1 cells. ND, not determined. (C) Huh7.5.1 and Hec1B/miR-122 cells were infected with HCVcc at MOIs of 0.1 and 1, respectively, incubated with 1% methylcellulose in DMEM containing 10% FCS for 72 h, fixed with 4% PFA, and subjected to immunofluorescence analysis using anti-NS5A antibody. (D) Hec1B/miR-122 and Huh7.5.1 cells were infected with HCVcc at MOIs of 1 and 0.1, respectively, and infectious titers in cells and supernatants were determined by a focus-forming assay at 72 h postinfection. (E) Huh7.5.1 and Hec1B/miR-122 cells were infected with HCVcc at MOIs of 0.1 and 1, respectively, fixed with 4% PFA, and subjected to immunofluorescence assay using anti-core protein antibody (green). Lipid droplets and cell nuclei were stained with BODIPY (red) and DAPI (blue), respectively. Asterisks indicate significant differences (**, $P < 0.01$) versus the results for Huh7.5.1 cells.

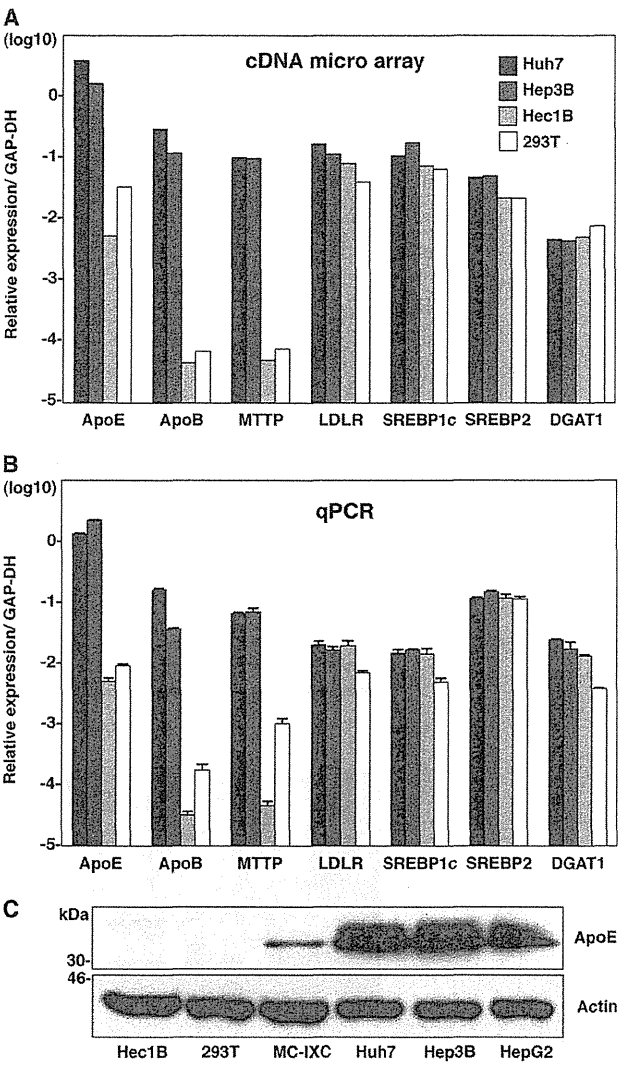

FIG 10 Expression of lipid metabolism-associated proteins in hepatic and nonhepatic cells. (A) Expression levels of ApoE, ApoB, MTTP, LDLR, SREBP1c, SREBP2, and DGAT1 were compared among hepatic (Huh7 and Hep3B) and nonhepatic (Hec1B and 293T) cells using cDNA microarray analyses. (B) Total RNA was extracted from the cells, and expression levels of ApoE, ApoB, MTTP, LDLR, SREBP1c, SREBP2, and DGAT1 gene were determined by qPCR. (C) Nonhepatic (Hec1B, 293T, and MC-IXC) and hepatic (Huh7, Hep3B, and HepG2) cells were subjected to immunoblotting using anti-ApoE antibody.

DISCUSSION

Although multiple epidemiological studies have revealed that HCV infection induces several EHMs, they have not well elucidated the molecular mechanisms of the EHMs induced by HCV infection (19). Indeed, HCVcc does not infect PBMCs (38). It has been shown that two neuroepithelioma cell lines permit HCVcc infection at low levels (17) and lymphotropic strains or quasispecies of HCV exist in infected individuals (12, 52). Furthermore, many molecules involved in the entry, replication, and assembly of HCVcc have been identified, although these molecules are not sufficient to explain the liver tropism of HCV. Recently, a liver-specific microRNA, miR-122, was shown to facilitate the efficient

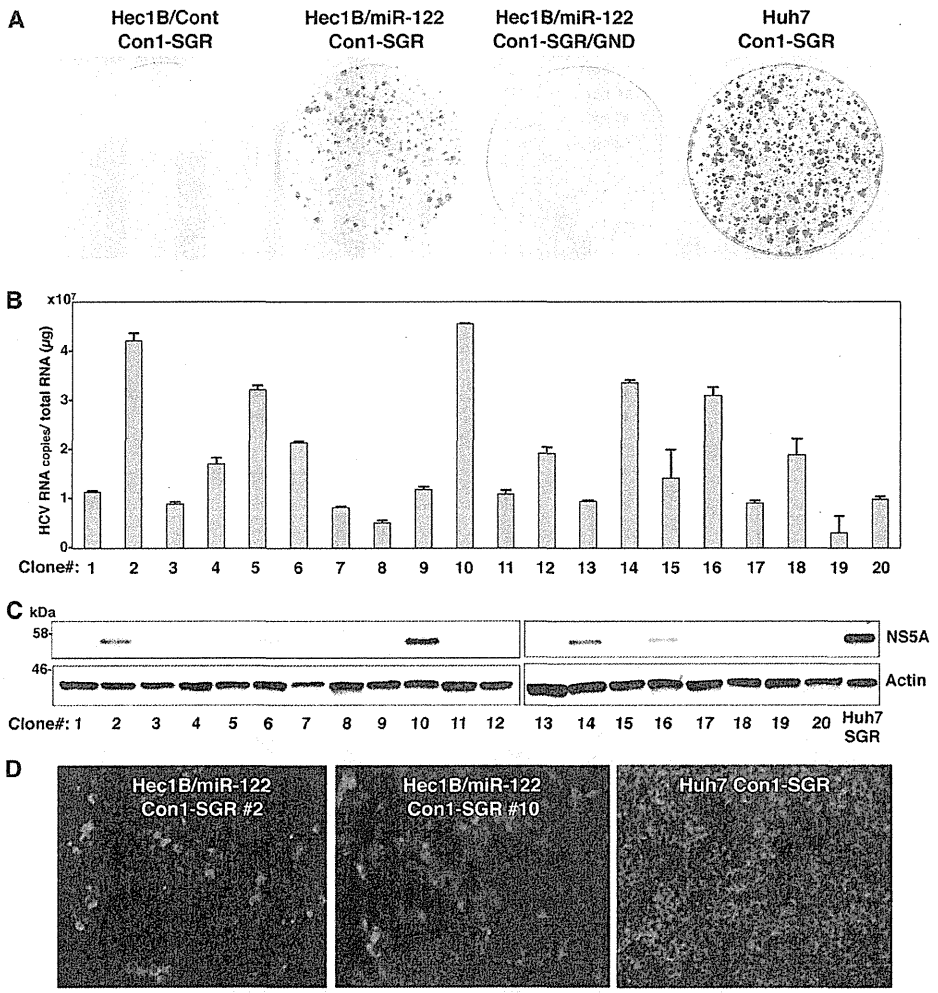

FIG 11 Establishment of Con1-based HCV replicon cells by using Hec1B cells. (A) WT or replication-defective SGR RNA of the HCV Con1 strain was electroporated into Hec1B/Cont, Hec1B/miR-122, and Huh7 cells, and the medium was replaced with DMEM containing 10% FCS and 1 mg/ml G418 at 24 h postelectroporation. Colonies were stained with crystal violet after 3 weeks of selection with G418. (B) Total RNAs of 20 selected clones were extracted and subjected to qRT-PCR. (C) The 20 SGR clones were subjected to immunoblotting using anti-NS5A antibody. Huh7-derived Con1-based SGR cells were used as a positive control. (D) NS5A proteins in SGR clones 2 and 10 were stained with appropriate antibodies and examined by fluorescence microscopy. Huh7-derived Con1-based SGR and parental Hec1B cells were used for positive and negative controls, respectively.

replication of HCV through a specific interaction with the complementary sequences in the 5′ UTR of HCV RNA (21, 25, 27, 36). In addition, exogenous expression of miR-122 facilitates the replication of SGR of the JFH1 strain in HEK293 cells (8) and the propagation of HCVcc in HepG2 and Hep3B nonpermissive hepatoma cells (29, 43), suggesting that the expression of miR-122 is required for the efficient replication of HCV. However, HCV replicon cells have also been established in HeLa and LI90 cells derived from stellate cells in which no exogenous miR-122 is expressed (30, 63). In this study, naïve Hec1B cells also exhibited a low level of replication upon infection with HCVcc (Fig. 4B), and this replication was resistant to treatment with an inhibitor of miR-122, LNA-miR-122 (Fig. 6C), suggesting that miR-122 expression is not a necessary condition but is required for the enhancement of HCV replication and that HCV is capable of replicating in nonhepatic cells in an miR-122-independent manner. Although the application of miR-122-specific LNAs to chronic hepatitis C patients is now in progress (32), further studies are needed to clarify the mechanisms underlying the miR-122-independent replication of HCV in more detail.

Although the importance of receptor-mediated entry in the cell tropism of HCV has been evaluated (16, 65), cDNA microarray databases, including the NextBio search engine, revealed that HCV receptor candidates, including hCD81, SR-BI, CLDN1, and OCLN, are highly expressed in many nonhepatic tissues. In addition, our current data and previous reports demonstrated that many nonhepatic cells permitted the entry of the pseudotype viruses bearing HCV envelope proteins, suggesting that other host factors must be involved in the cell tropism of HCV to human hepatocytes (4, 17, 54, 61). The data in this study suggest that miR-122 expression and functional lipid metabolism play crucial roles in the determination of an efficient propagation of HCV *in vitro*. On the other hand, previous studies showed the compartmentalization of genetic variation in HCV between hepatic and

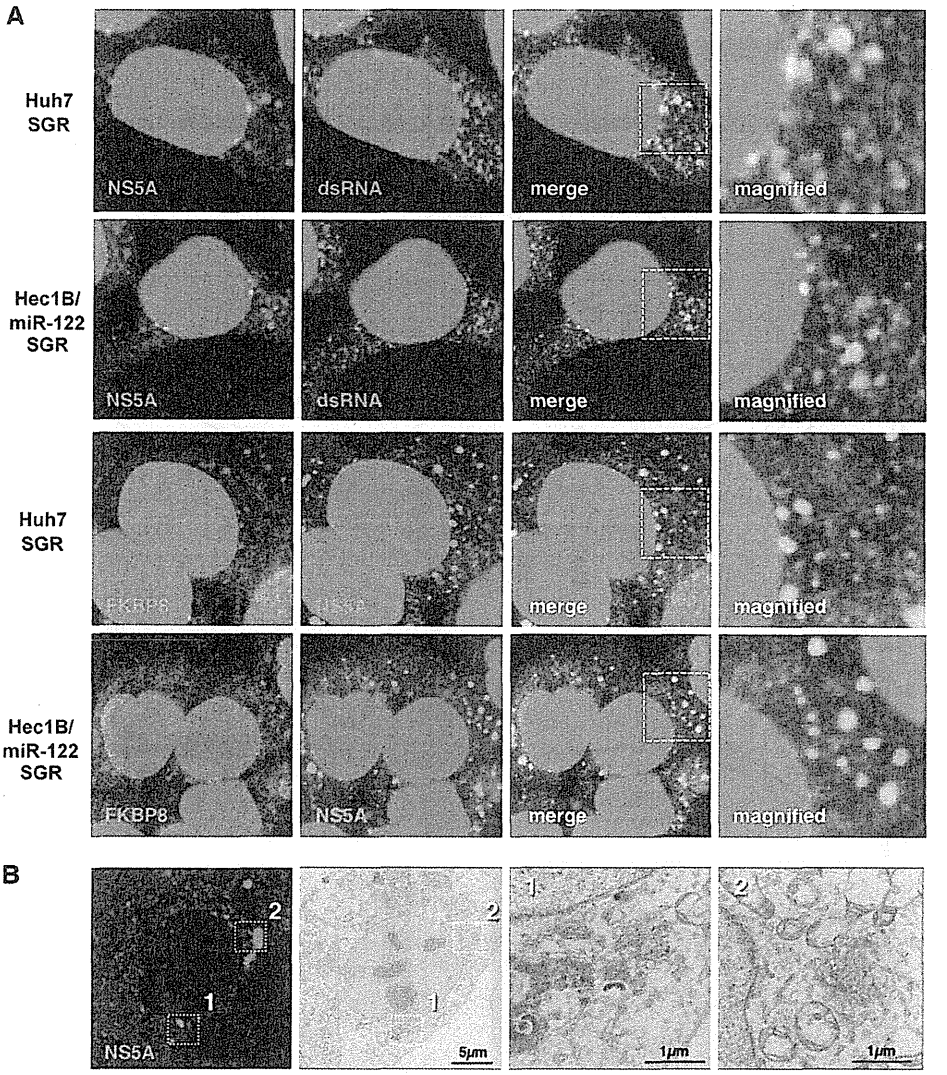

FIG 12 Replication complex in Hec1B/miR-122 replicon cells. (A) Huh7 and Hec1B/miR-122 cells harboring the Con1 SGR RNA were fixed, permeabilized, and stained with antibodies to NS5A and dsRNA or FKBP8. The boxed areas in the merged images were magnified, and the images are displayed on the right. (B) Hec1B-derived Con1 SGR cells were stained with anti-NS5A antibody. Identical fields were observed under EM by using the correlative FM-EM technique. The boxed areas are magnified, and the images displayed on the right.

nonhepatic tissues, suggesting that HCV is capable of replicating in nonhepatic tissues expressing either miR-122, ApoE, ApoB, or MTTP (52). Collectively, these results suggest that entry receptors, miR-122, and functional lipid metabolism are mainly involved in the regulation of internalization, RNA replication, and assembly of HCV, respectively, and are important factors in determining the cell tropism of HCV to hepatocytes. On the other hand, it might be feasible to speculate that EHMs observed in chronic hepatitis C patients are caused by an incomplete miR-122-independent propagation of HCV in nonhepatic cells.

In spite of the efficient replication of HCV in Hec1B and 293T-CLDN cells expressing miR-122, no infectious particle was detected, in contrast to the case with hepatic cells (Fig. 9), suggesting the involvement of liver-specific host factors and/or machineries in the assembly of infectious particles. In general, the liver plays a major role in lipid metabolism, such as in fatty acid and lipoprotein syntheses (9), and many reports have indicated the involvement of lipid metabolism, especially triglyceride metabolism, in the assembly and budding of HCV particles. Lipid droplets, MTTP, ApoB, and ApoE have been shown to participate in the assembly and secretion of infectious particles of HCVcc in Huh7 cells (20, 23, 26, 40). In the current analyses, there were fewer lipid droplets and the expression levels of ApoE, ApoB, and MTTP were lower in nonhepatic cells than in hepatic cells. Although minus-strand HCV RNA and viral proteins were detected in nonhepatic cells (33, 60), it was shown that the recurrence of HCV after liver transplantation for patients with HCV-induced liver diseases was mainly caused by HCV variants generated in the liver but not in nonhepatic tissues (50). These results support the notion that replication of HCV RNA in nonhepatic cells is unlikely to be a reservoir for persistent infection, due to the lack of infectious particle formation.

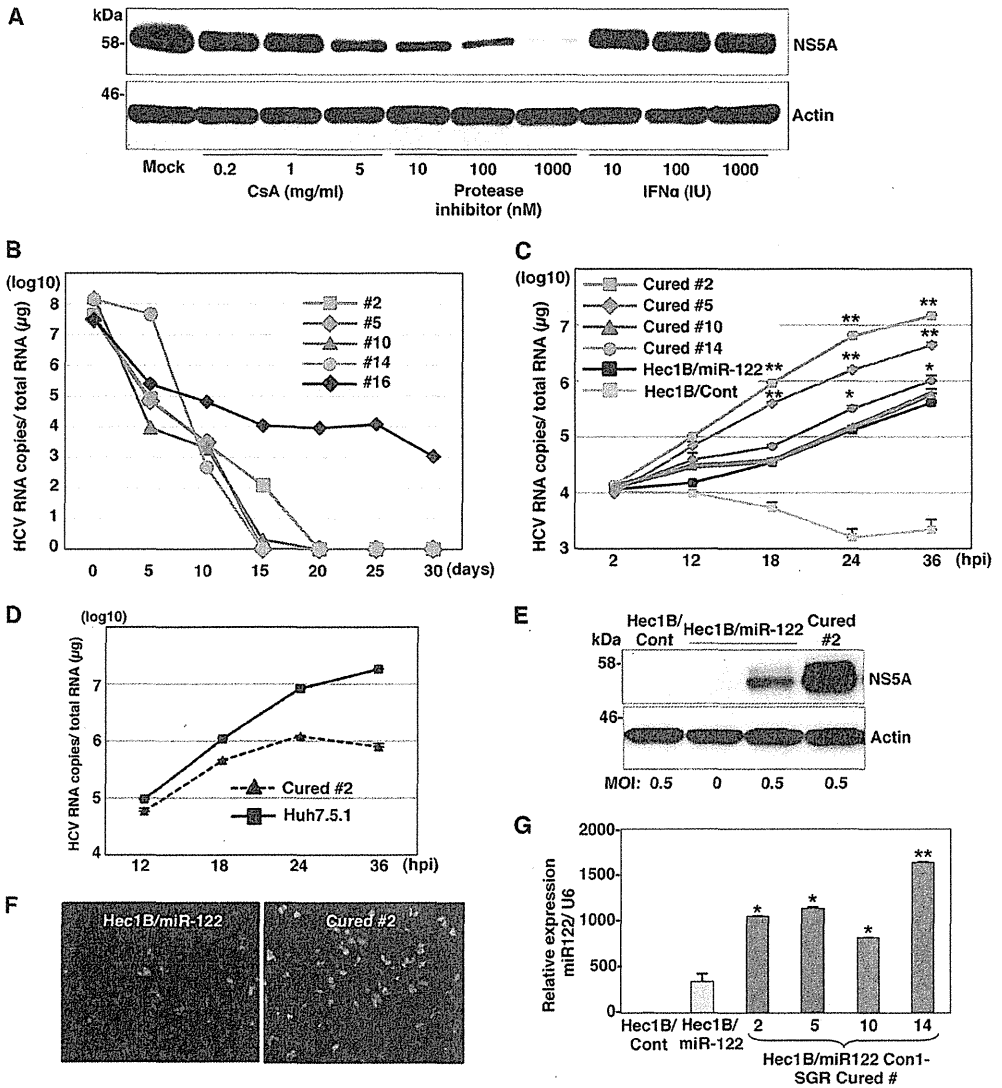

FIG 13 miR-122 is a crucial determinant for the efficient replication of HCVcc and replicon RNA. (A) Hec1B Con1 replicon clone 2 was treated with stepwise concentrations of cyclosporine (CsA; 0.2, 1, and 5 μg/ml), NS3/4A protease inhibitor (10, 100, and 1,000 nM), or IFN-α (10, 100, and 1,000 IU) and subjected to immunoblotting using anti-NS5A antibody at 48 h posttreatment. (B) Five Con1-based SGR clones were treated with the combination of 1 μg/ml cyclosporine and 100 nM HCV protease inhibitor to eliminate the HCV genome. Intracellular HCV RNA levels at 5, 10, 15, 20, 25, and 30 days posttreatment were determined by qRT-PCR analysis. (C) HCVcc was inoculated with Hec1B/Cont, parental Hec1B/miR-122, and Hec1B-based cured cells (clones 2, 5, 10, and 14) at an MOI of 1. Intracellular HCV RNA levels at 2, 12, 18, 24, and 36 h postinfection were determined by qRT-PCR analysis. (D) HCVcc was inoculated into Huh7.5.1 and Hec1B/miR-122 cured clone 2 cells at an MOI of 1. Intracellular HCV RNA levels were determined by qRT-PCR at 12, 24, 36, and 48 h postinfection. (E and F) Hec1B/Cont, parental Hec1B/miR-122, and cured cells of clone 2 were infected with HCVcc at an MOI of 0.5. After 48 h, the cells were subjected to immunoblotting and immunofluorescence analyses using appropriate antibodies. (G) Total miRNAs were extracted from Hec1B/Cont (white), parental Hec1B-miR-122 cells (gray), and four cured cell clones (black). miR-122 expression levels in these cells were determined by qRT-PCR analysis. Asterisks indicate significant differences (*, $P < 0.05$; **, $P < 0.01$) versus the results for parental Hec1B/miR-122 cells.

The endogenous expression of miR-122 is hardly detected in Hec1B cells, in contrast to the abundant expression of miR-122 in Huh7 cells. Therefore, more accurate analyses of the biological significance of the interaction between miR-122 and the 5′ UTR on the replication of HCVcc in Hec1B could be possible by introducing mutations not only into viruses but also into miR-122. Replication of HCVcc and a mutant virus bearing two mutations in the 5′ UTR (HCVcc-M2) was observed in Hec1B cells expressing WT and MT miR-122, respectively, although the level of replication was lower in cells infected with HCVcc-M2 than in those infected with HCVcc, probably due to the mutations in the 5′ UTR (Fig. 8F). In contrast, a mutant virus (HCVcc-M1) bearing a mutation in site 1 alone exhibited efficient replication in Hec1B cells expressing both WT and MT miR-122 comparable to the replication level of the wild-type virus in cells expressing WT miR-122. Furthermore, the replication level of HCVcc-M1 was low in Hec1B cells expressing either WT or MT miR-122, suggesting that interaction between miR-122 and either of the seed sequence-binding sites in the 5′ UTR has an equal ability to enhance the replication of the HCV genome. However, it was shown that the

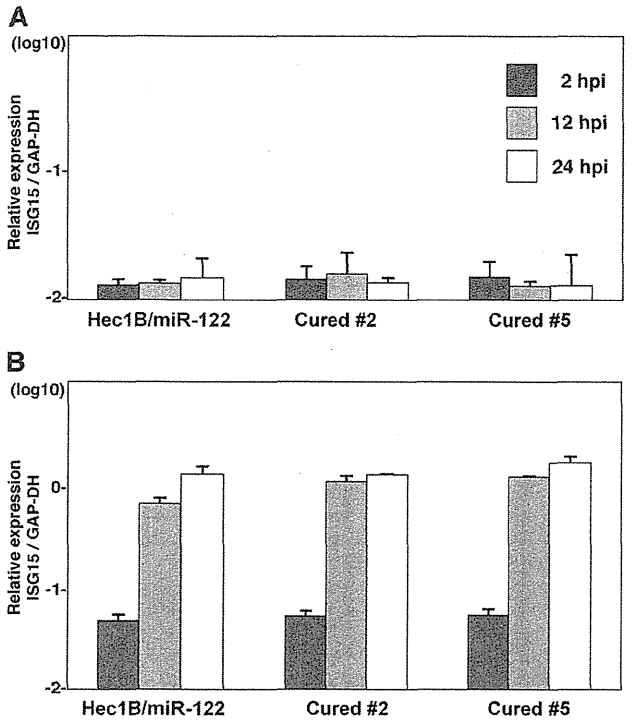

FIG 14 Innate immune responses in parental and cured Hec1B/miR-122 cells. Parental and cured Hec1B/miR-122 cells were stimulated with 100 U of IFN-α (A) or VSV (B). The expression levels of IFN-stimulated gene 15 (ISG15) were determined by qRT-PCR at 2, 12, and 24 h posttreatment.

ability of miR-122 to promote the growth of a laboratory strain of HCV (HJ3-5) is dependent upon its direct interaction with both seed sequence-binding sites in the 5′ UTR and that the binding to site 1 is more important for efficient replication than the binding to site 2 (25). Recently, it was shown that the binding of miR-122 to the 5′ UTR of the HCV genome masks the 5′-terminal sequences of the viral genome through the 3′ overhanging nucleotides of miR-122 (36). It is necessary to evaluate the importance of this enhancement mechanism on mutant HCVcc infection in Hec1B cells.

In summary, we demonstrated that HCV is capable of replicating at a low level in nonhepatic cells and that exogenous expression of miR-122 facilitates efficient viral replication but not the production of infectious particles, probably due to the lack of hepatocytic lipid metabolism in nonhepatic cell lines. These results suggest that miR-122 plays a crucial role in determination of the cell tropism of HCV and the possible involvement of incomplete propagation of HCV in the development of EHM in hepatitis C patients.

ACKNOWLEDGMENTS

We thank M. Tomiyama for her secretarial work. We also thank C. Oneyama, M. Hijikata, T. Wakita, and F. Chisari for providing experimental materials. We also thank H. Ohmori for her excellent technical assistance.

This work was supported in part by grants-in-aid from the Japanese Ministry of Health, Labor, and Welfare (Research on Hepatitis); the Japanese Ministry of Education, Culture, Sports, Science, and Technology; and the Osaka University Global Center of Excellence Program.

REFERENCES

1. Bartel DP. 2009. MicroRNAs: target recognition and regulatory functions. Cell 136:215–233.
2. Blight KJ, McKeating JA, Rice CM. 2002. Highly permissive cell lines for subgenomic and genomic hepatitis C virus RNA replication. J. Virol. 76: 13001–13014.
3. Bukh J. 2004. A critical role for the chimpanzee model in the study of hepatitis C. Hepatology 39:1469–1475.
4. Burgel B, et al. 2011. Hepatitis C virus enters human peripheral neuroblastoma cells—evidence for extra-hepatic cells sustaining hepatitis C virus penetration. J. Viral Hepat. 18:562–570.
5. Burns DM, D'Ambrogio A, Nottrott S, Richter JD. 2011. CPEB and two poly(A) polymerases control miR-122 stability and p53 mRNA translation. Nature 473:105–108.
6. Calleja JL, et al. 1999. Sustained response to interferon-alpha or to interferon-alpha plus ribavirin in hepatitis C virus-associated symptomatic mixed cryoglobulinaemia. Aliment. Pharmacol. Ther. 13:1179–1186.
7. Castoldi M, et al. 2011. The liver-specific microRNA miR-122 controls systemic iron homeostasis in mice. J. Clin. Invest. 121:1386–1396.
8. Chang J, et al. 2008. Liver-specific microRNA miR-122 enhances the replication of hepatitis C virus in nonhepatic cells. J. Virol. 82:8215–8223.
9. Coppack SW, Jensen MD, Miles JM. 1994. In vivo regulation of lipolysis in humans. J. Lipid Res. 35:177–193.
10. Cun W, Jiang J, Luo G. 2010. The C-terminal alpha-helix domain of apolipoprotein E is required for interaction with nonstructural protein 5A and assembly of hepatitis C virus. J. Virol. 84:11532–11541.
11. Daly C, Reich NC. 1993. Double-stranded RNA activates novel factors that bind to the interferon-stimulated response element. Mol. Cell. Biol. 13:3756–3764.
12. Di Liberto G, et al. 2006. Clinical and therapeutic implications of hepatitis C virus compartmentalization. Gastroenterology 131:76–84.
13. Egger D, et al. 2002. Expression of hepatitis C virus proteins induces distinct membrane alterations including a candidate viral replication complex. J. Virol. 76:5974–5984.
14. Ehrhardt M, et al. 2011. Profound differences of microRNA expression patterns in hepatocytes and hepatoma cell lines commonly used in hepatitis C virus studies. Hepatology 54:1112–1113.
15. Elmen J, et al. 2008. LNA-mediated microRNA silencing in non-human primates. Nature 452:896–899.
16. Evans MJ, et al. 2007. Claudin-1 is a hepatitis C virus co-receptor required for a late step in entry. Nature 446:801–805.
17. Fletcher NF, et al. 2010. Hepatitis C virus infection of neuroepithelioma cell lines. Gastroenterology 139:1365–1374.
18. Fukuhara T, et al. 2011. Intracellular delivery of serum-derived hepatitis C virus. Microbes Infect. 13:405–412.
19. Galossi A, Guarisco R, Bellis L, Puoti C. 2007. Extrahepatic manifestations of chronic HCV infection. J. Gastrointestin. Liver Dis. 16:65–73.
20. Gastaminza P, et al. 2008. Cellular determinants of hepatitis C virus assembly, maturation, degradation, and secretion. J. Virol. 82:2120–2129.
21. Henke JI, et al. 2008. microRNA-122 stimulates translation of hepatitis C virus RNA. EMBO J. 27:3300–3310.
22. Herker E, et al. 2010. Efficient hepatitis C virus particle formation requires diacylglycerol acyltransferase-1. Nat. Med. 16:1295–1298.
23. Hishiki T, et al. 2010. Infectivity of hepatitis C virus is influenced by association with apolipoprotein E isoforms. J. Virol. 84:12048–12057.
24. Huntzinger E, Izaurralde E. 2011. Gene silencing by microRNAs: contributions of translational repression and mRNA decay. Nat. Rev. Genet. 12:99–110.
25. Jangra RK, Yi M, Lemon SM. 2010. Regulation of hepatitis C virus translation and infectious virus production by the microRNA miR-122. J. Virol. 84:6615–6625.
26. Jiang J, Luo G. 2009. Apolipoprotein E but not B is required for the formation of infectious hepatitis C virus particles. J. Virol. 83:12680–12691.
27. Jopling CL, Schutz S, Sarnow P. 2008. Position-dependent function for a tandem microRNA miR-122-binding site located in the hepatitis C virus RNA genome. Cell Host Microbe 4:77–85.
28. Jopling CL, Yi M, Lancaster AM, Lemon SM, Sarnow P. 2005. Modulation of hepatitis C virus RNA abundance by a liver-specific microRNA. Science 309:1577–1581.
29. Kambara H, et al. 2012. Establishment of a novel permissive cell line for

propagation of hepatitis C virus by the expression of microRNA miR122. J. Virol. 86:1382–1393.
30. **Kato T, et al.** 2005. Nonhepatic cell lines HeLa and 293 support efficient replication of the hepatitis C virus genotype 2a subgenomic replicon. J. Virol. 79:592–596.
31. **Kupershmidt IQ, et al.** 2010. Ontology-based meta-analysis of global collections of high-throughput public data. PLoS One 5:e13066. doi: 10.1371/journal.pone.0013066.
32. **Lanford RE, et al.** 2010. Therapeutic silencing of microRNA-122 in primates with chronic hepatitis C virus infection. Science 327:198–201.
33. **Lerat H, et al.** 1996. Specific detection of hepatitis C virus minus strand RNA in hematopoietic cells. J. Clin. Invest. 97:845–851.
34. **Lin C, et al.** 2004. In vitro resistance studies of hepatitis C virus serine protease inhibitors, VX-950 and BILN 2061: structural analysis indicates different resistance mechanisms. J. Biol. Chem. 279:17508–17514.
35. **Lin LT, et al.** 2010. Replication of subgenomic hepatitis C virus replicons in mouse fibroblasts is facilitated by deletion of interferon regulatory factor 3 and expression of liver-specific microRNA 122. J. Virol. 84:9170–9180.
36. **Machlin ES, Sarnow P, Sagan SM.** 2011. Masking the 5′ terminal nucleotides of the hepatitis C virus genome by an unconventional microRNA-target RNA complex. Proc. Natl. Acad. Sci. U. S. A. 108:3193–3198.
37. **Manns MP, et al.** 2001. Peginterferon alfa-2b plus ribavirin compared with interferon alfa-2b plus ribavirin for initial treatment of chronic hepatitis C: a randomised trial. Lancet 358:958–965.
38. **Marukian S, et al.** 2008. Cell culture-produced hepatitis C virus does not infect peripheral blood mononuclear cells. Hepatology 48:1843–1850.
39. **Masaki T, et al.** 2010. Production of infectious hepatitis C virus by using RNA polymerase I-mediated transcription. J. Virol. 84:5824–5835.
40. **Miyanari Y, et al.** 2007. The lipid droplet is an important organelle for hepatitis C virus production. Nat. Cell Biol. 9:1089–1097.
41. **Moriishi K, et al.** 2010. Involvement of PA28gamma in the propagation of hepatitis C virus. Hepatology 52:411–420.
42. **Morris T, Robertson B, Gallagher M.** 1996. Rapid reverse transcription-PCR detection of hepatitis C virus RNA in serum by using the TaqMan fluorogenic detection system. J. Clin. Microbiol. 34:2933–2936.
43. **Narbus CM, et al.** 2011. HepG2 cells expressing microRNA miR-122 support the entire hepatitis C virus life cycle. J. Virol. 85:12087–12092.
44. **Okamoto T, et al.** 2006. Hepatitis C virus RNA replication is regulated by FKBP8 and Hsp90. EMBO J. 25:5015–5025.
45. **Okamoto T, et al.** 2008. A single-amino-acid mutation in hepatitis C virus NS5A disrupting FKBP8 interaction impairs viral replication. J. Virol. 82:3480–3489.
46. **Pawlotsky JM, Chevaliez S, McHutchison JG.** 2007. The hepatitis C virus life cycle as a target for new antiviral therapies. Gastroenterology 132: 1979–1998.
47. **Pietschmann T, et al.** 2002. Persistent and transient replication of full-length hepatitis C virus genomes in cell culture. J. Virol. 76:4008–4021.
48. **Pileri P, et al.** 1998. Binding of hepatitis C virus to CD81. Science 282: 938–941.
49. **Ploss A, et al.** 2009. Human occludin is a hepatitis C virus entry factor required for infection of mouse cells. Nature 457:882–886.
50. **Ramirez S, et al.** 2009. Hepatitis C virus compartmentalization and infection recurrence after liver transplantation. Am. J. Transplant. 9:1591–1601.
51. **Rieder CL, Bowser SS.** 1985. Correlative immunofluorescence and electron microscopy on the same section of Epon-embedded material. J. Histochem. Cytochem. 33:165–171.
52. **Roque-Afonso AM, et al.** 2005. Compartmentalization of hepatitis C virus genotypes between plasma and peripheral blood mononuclear cells. J. Virol. 79:6349–6357.
53. **Russell RS, et al.** 2008. Advantages of a single-cycle production assay to study cell culture-adaptive mutations of hepatitis C virus. Proc. Natl. Acad. Sci. U. S. A. 105:4370–4375.
54. **Sainz B, Jr, et al.** 2012. Identification of the Niemann-Pick C1-like 1 cholesterol absorption receptor as a new hepatitis C virus entry factor. Nat. Med. 18:281–285.
55. **Sarrazin C, et al.** 2007. Dynamic hepatitis C virus genotypic and phenotypic changes in patients treated with the protease inhibitor telaprevir. Gastroenterology 132:1767–1777.
56. **Scarselli E, et al.** 2002. The human scavenger receptor class B type I is a novel candidate receptor for the hepatitis C virus. EMBO J. 21:5017–5025.
57. **Seeff LB.** 2002. Natural history of chronic hepatitis C. Hepatology 36:S35–S46. doi:10.1002/hep.1840360706.
58. **Sumpter RJ, et al.** 2005. Regulating intracellular antiviral defense and permissiveness to hepatitis C virus RNA replication through a cellular RNA helicase, RIG-I. J. Virol. 79:2689–2699.
59. **Taguwa S, et al.** 2009. Cochaperone activity of human butyrate-induced transcript 1 facilitates hepatitis C virus replication through an Hsp90-dependent pathway. J. Virol. 83:10427–10436.
60. **Takyar ST, Li D, Wang Y, Trowbridge R, Gowans EJ.** 2000. Specific detection of minus-strand hepatitis C virus RNA by reverse-transcription polymerase chain reaction on polyA(+)-purified RNA. Hepatology 32: 382–387.
61. **Tani H, et al.** 2007. Replication-competent recombinant vesicular stomatitis virus encoding hepatitis C virus envelope proteins. J. Virol. 81: 8601–8612.
62. **Wakita T, et al.** 2005. Production of infectious hepatitis C virus in tissue culture from a cloned viral genome. Nat. Med. 11:791–796.
63. **Watanabe N, et al.** 2011. Hepatitis C virus RNA replication in human stellate cells regulates gene expression of extracellular matrix-related molecules. Biochem. Biophys. Res. Commun. 407:135–140.
64. **Wilkinson J, Radkowski M, Laskus T.** 2009. Hepatitis C virus neuroinvasion: identification of infected cells. J. Virol. 83:1312–1319.
65. **Yang W, et al.** 2008. Correlation of the tight junction-like distribution of claudin-1 to the cellular tropism of hepatitis C virus. J. Biol. Chem. 283: 8643–8653.
66. **Zhong J, et al.** 2005. Robust hepatitis C virus infection in vitro. Proc. Natl. Acad. Sci. U. S. A. 102:9294–9299.

JVI
Journals.ASM.org

CD44 Participates in IP-10 Induction in Cells in Which Hepatitis C Virus RNA Is Replicating, through an Interaction with Toll-Like Receptor 2 and Hyaluronan

Takayuki Abe,[a]* Takasuke Fukuhara,[a] Xiauyu Wen,[a]* Akinori Ninomiya,[a] Kohji Moriishi,[c] Yoshihiko Maehara,[d] Osamu Takeuchi,[b] Taro Kawai,[b] Shizuo Akira,[b] and Yoshiharu Matsuura[a]

Department of Molecular Virology, Research Institute for Microbial Diseases,[a] and Laboratory of Host Defense, WPI Immunology Frontier Research Center,[b] Osaka University, Osaka, Department of Microbiology, Faculty of Medicine, Yamanashi University, Yamanashi,[c] and Department of Surgery and Science, Graduate School of Medical Sciences, Kyushu University, Fukuoka, Japan[d]

The mechanisms of induction of liver injury during chronic infection with hepatitis C virus (HCV) are not well understood. Gamma interferon (IFN-γ)-inducible protein 10 (IP-10), a member of the CXC chemokine family, is expressed in the liver of chronic hepatitis C (CHC) patients and selectively recruits activated T cells to the sites of inflammation. Recently, it was shown that a low plasma concentration of IP-10 in CHC patients was closely associated with the outcome of antiviral therapy. In this study, we examined the role of the Toll-like receptor (TLR) pathway on IP-10 production in cells replicating HCV. Among the CXC chemokines, the expression of IP-10 was specifically increased in cells replicating HCV upon stimulation with conventional TLR2 ligands. The enhancement of IP-10 production upon stimulation with TLR2 ligands in cells replicating HCV induced CD44 expression. CD44 is a broadly distributed type I transmembrane glycoprotein and a receptor for the glycosaminoglycan hyaluronan (HA). In CHC patients, the expression of HA in serum has been shown to increase in accord with the progression of liver fibrosis, and HA also works as a ligand for TLR2. In the present study, IP-10 production upon HA stimulation was dependent on the expression of TLR2 and CD44, and a direct association between TLR2 and CD44 was observed. These results suggest that endogenous expression of HA in hepatocytes in CHC patients participates in IP-10 production through an engagement of TLR2 and CD44.

Hepatitis C virus (HCV) infects 170 million people worldwide and frequently leads to the development of cirrhosis and hepatocellular carcinoma (32). The current combination therapy of pegylated interferon (IFN) and ribavirin is effective in fewer than 50% of patients infected with HCV of genotype 1. Histological analyses of the liver biopsy specimens of chronic hepatitis C (CHC) patients have revealed the infiltration of mononuclear cells, including T and B lymphocytes, natural killer (NK) and NKT cells, and virus-specific cytotoxic T lymphocytes (2, 26, 42, 47). Long-term infection by HCV is associated with progressive infiltration of the liver parenchyma by the mononuclear cells, fibrosis, cirrhosis, and, finally, the development of hepatocellular carcinoma. Although the factors that regulate the recruitment of mononuclear cells and the other components of the inflammatory response to the HCV-infected liver cells are not well characterized, it has been hypothesized that chemokines and other inflammatory cytokines play fundamental roles in the immune cell recruitment.

Chemokines, small chemotactic cytokines (approximately 8 to 10 kDa) that act to guide leukocytes to sites of inflammation, are important determinants of the development of intrahepatic inflammation in chronic HCV infection (16). Although chemokines play crucial roles in viral elimination, persistent expression of chemokines may induce tissue damage and inflammation in chronic infection. CXCR3 is a receptor for the CXC chemokines, including IP-10 (also known as CXCL10), MIG (also known as CXCL9), and I-TAC (also known as CXCL11). Recent studies have shown that the CXCR3 ligands are elevated in the livers and sera of CHC patients (12–14, 17, 33, 36, 40, 49), and IP-10 was shown to correlate with treatment response. In addition, several studies suggested a significant association between the expression of the CXC chemokines and the development of progressive liver injury in CHC patients (23, 49). In CHC patients, these chemokines are expressed in hepatocytes, hepatic stellate cells, and sinusoidal endothelial cells (12, 14, 33, 42, 49), and the majority of intrahepatic mononuclear cells express CXCR3, suggesting that the CXC chemokine network plays a pivotal role in the migration of mononuclear cells to the liver and in the subsequent intrahepatic inflammation.

Among chemokines, IP-10 plays a central role in liver inflammation, and it is expressed in the liver of hepatitis C patients (12, 33, 42). Several independent studies indicate that elevated plasma levels of IP-10 predict the failure of combination therapy (3, 5, 40). In addition, a recent study suggests that IP-10 in the plasma of many hepatitis C patients is cleaved by DPP4 (also known as CD26) and that the truncated IP-10 works as an IP-10 receptor antagonist (4). In contrast to these clinical observations, little is known about the expression of the CXC chemokines in cells replicating HCV.

Production of the inflammatory chemokines upon viral infec-

Received 21 November 2011 Accepted 23 March 2012
Published ahead of print 4 April 2012
Address correspondence to Yoshiharu Matsuura, matsuura@biken.osaka-u.ac.jp.
* Present address: Takayuki Abe, Department of Medicine, University of Miami School of Medicine, Miami, Florida, USA; Xiauyu Wen, Department of Hepatology, The First Hospital of Jilin University, Changchun, Jilin Province, China.

doi:10.1128/JVI.06872-11

tion is also crucial for the induction of innate immunity through the activation of pattern recognition receptors (PRR), including Toll-like receptors (TLR) and RIG-I-like receptors (RLR) (44). TLR play an important role in the recognition of a wide variety of pathogens and their components, while RLR, including RIG-I and MDA5, sensitize cells in response to double-stranded RNA (dsRNA) generated by viral infection or to poly(I·C). Various proinflammatory cytokines and chemokines are activated by the PRR through the translocation of transcription factors, such as IFN regulatory factor (IRF) and NF-κB, into the nucleus and binding to their cognate promoter elements together with other transcription factors.

In this study, we have examined the role of the TLR pathway on the production of the CXC chemokines in human liver cell lines replicating HCV RNA. Among the CXC chemokines, IP-10 production was specifically enhanced in cells replicating HCV upon stimulation with conventional TLR2 ligands. Moreover, we identified CD44, a receptor for the glycosaminoglycan hyaluronan (HA) (38), as a molecule involved in IP-10 production in the HCV-replicating cells. The cell surface expression of CD44 was also upregulated in the cells harboring HCV replicons of genotypes 1b and 2a, and IP-10 production was enhanced in cells replicating HCV upon stimulation with HA. Importantly, HA also works as a ligand for TLR2 (41), and HA expression in serum is increased in CHC patients in accord with the progression of liver fibrosis (9, 30, 35, 45, 48). These results suggest that the production of IP-10 is enhanced by endogenous HA in hepatocytes in CHC patients through an interaction with TLR2 and CD44.

MATERIALS AND METHODS

Cells and viruses. Huh7OK1 cells that exhibit high susceptibility to infectious cell culture-adapted HCV clone (HCVcc) propagation (34), Huh7 cells, and 293T cells were maintained in Dulbecco's modified Eagle's medium (DMEM) (Sigma, St. Louis, MO) supplemented with 10% fetal calf serum (FCS). Huh7 cells harboring an HCV subgenomic RNA replicon of genotype 1b (Con1 strain) (28) or 2a (JFH1 strain) were cultured in DMEM supplemented with 10% FCS, 1 mg/ml G418 (Nacalai Tesque, Kyoto, Japan), and nonessential amino acids. Human normal hepatocytes and human liver sinusoidal endothelial cells were purchased from TaKaRa Bio, Inc. (Shiga, Japan) and maintained in primary hepatocytes and endothelial selective medium (TaKaRa Bio), respectively. Huh7 cells harboring a Japanese encephalitis virus (JEV) subgenomic RNA replicon (Nakayama strain) were cultured in DMEM supplemented with 10% FCS and 1 μg/ml puromycin (InvivoGen, San Diego, CA). The cells were cultured at 37°C in a humidified atmosphere with 5% CO_2. The infectious RNA of the JFH1 strain was introduced into Huh7OK1 cells, and the infectious titers were expressed as focus-forming units (FFU) (46).

Plasmids and reagents. The cDNA fragment encoding CD44 was kindly provided by U. Günthert (University of Basel, Switzerland) (31) and subcloned into pcDNA3.1-C-myc-His (Invitrogen, Carlsbad, CA). The N-terminal or C-terminal deletion mutant of CD44 was amplified by PCR using *Pfu* Turbo DNA polymerase (Stratagene, La Jolla, CA) and subcloned into pcDNA3.1-C-myc-His. The cDNA fragment encoding the full-length human TLR2 was amplified by reverse transcription (RT)-PCR from total RNA of THP-1 cells and subcloned into pFlagCMV-1 (Sigma). The C-terminal deletion mutant of TLR2 was amplified by PCR using *Pfu* Turbo DNA polymerase (Stratagene) and subcloned into pFlagCMV-1. All PCR products were confirmed by sequencing with an ABI PRISM 3100 genetic analyzer (Applied Biosystems, Tokyo, Japan). Lipopolysaccharide (LPS) derived from *Salmonella enterica* subsp. *enterica* serovar Minnesota (Re-595) and peptidoglycans (PGN) derived from *Staphylococcus aureus* were purchased from Sigma. FSL-1 (a synthetic lipopeptide derived from *Mycoplasma salivarium*), Pam2CSK (a synthetic diacylated lipopeptide), Pam3CSK (a tripalmitoylated lipopeptide), phosphorothioate-stabilized human CpG (hCpG) oligodeoxynucleotides (ODN 2006) (TCG-TCG-TTT-TGT-CGT-TTT-GTC-GTT), R-837, and poly(I·C) were purchased from InvivoGen. Purified hyaluronan from human umbilical cords was purchased from Calbiochem (Darmstadt, Germany). The recombinant human alpha interferon (IFN-α) and IFN-γ were purchased from PBL Biomedical Laboratories (New Brunswick, NJ). The Quantikine ELISA (enzyme-linked immunosorbent assay) human CXCL10/IP-10 immunoassay was purchased from R&D Systems, Inc. (Minneapolis, MN). The HCV NS3/-4A protease inhibitor BILN2061 was purchased from Acme Bioscience (Belmont, CA). Lack of contamination of endotoxin (<0.01 endotoxin units/ml) in the regents, including virus stocks, recombinant proteins, and all ligands, was confirmed by using a Pyrodick endotoxin measure kit (Seikagaku Co., Tokyo, Japan).

Binding of recombinant CD44s to TLR2 or ligands. To generate a C-terminal deletion mutant of TLR2 (comprised of amino acid residues from 1 to 587) or CD44 (comprised of amino acid residues from 1 to 223), each of the cDNAs encoding N-terminally FLAG-tagged TLR2 (TLR2ΔTM) or C-terminally His-tagged CD44 (CD44ΔTM) were subcloned into pFastBac (Invitrogen), and recombinant baculoviruses possessing the cDNA were produced by using a Bac-to-Bac baculovirus expression system according to the manufacturer's instructions (Invitrogen). At 3 days after infection, TLR2ΔTM and CD44ΔTM proteins were purified from the culture supernatants and cell lysates by using column chromatography with nickel-nitrilotriacetic acid beads (Qiagen, Valencia, CA) and anti-FLAG M2 affinity gel (Sigma) according to the respective manufacturer's instructions. The protein concentrations were determined by using a Micro BCA (bicinchoninic acid) protein assay kit (Pierce, Rockford, IL). One hundred microliters of TLR2ΔTM (20 μg/ml), HA (50 μg/ml), PGN (40 μg/ml), LPS (40 μg/ml), or bovine serum albumin (BSA) (50 μg/ml) was added to a 96-well microtiter plate (Nunc Maxisorp P/N; Nalge Nunc International, Rochester, NY) and incubated at 4°C overnight. Nonspecific binding was blocked by incubating with phosphate-buffered saline (PBS) containing 2% FCS (PBSF) at room temperature for 1 h, followed by washing with PBS containing 0.02% Tween 20 (PBST) and incubation with various concentrations of CD44ΔTM in the PBSF at room temperature for 1 h. The wells were washed with PBST and incubated for 1 h with an antihexahistidine monoclonal antibody (Santa Cruz Biotechnology, Santa Cruz, CA), followed by incubation with horseradish peroxidase (HRP)-conjugated goat anti-mouse IgG, and then supplemented with *o*-phenylenediamine after washing with PBST. The binding of the CD44ΔTM to TLR2ΔTM, PGN, LPS, or BSA was determined by measuring the absorbance at 450 nm.

Immunoprecipitation and immunoblotting. Cells were transfected with the plasmids by the lipofection method, harvested at 48 h posttransfection, washed three times with ice-cold PBS, and suspended in 0.4 ml lysis buffer containing 20 mM Tris-HCl (pH 7.4), 135 mM NaCl, 1% Triton X-100, 1% glycerol, and protease inhibitor cocktail tablets (Roche Molecular Biochemicals, Mannheim, Germany). Cell lysates were incubated for 30 min at 4°C and centrifuged at 14,000 × *g* for 15 min at 4°C. The supernatant was immunoprecipitated with mouse monoclonal anti-FLAG M2 and protein G-Sepharose 4B fast flow beads (Amersham Pharmacia Biotech, Franklin Lakes, NJ), and the precipitates were washed with Tris-buffered saline containing 20 mM Tris-HCl (pH 7.4), 135 mM NaCl, and 0.05% Tween 20 (TBST). The proteins bound to the beads were boiled in 20 μl of sample buffer, subjected to sodium dodecyl sulfate–12.5% polyacrylamide gel electrophoresis (SDS-PAGE), and transferred to polyvinylidene difluoride membranes (Millipore, Tokyo, Japan). These membranes were blocked with TBST containing 5% skim milk and incubated with mouse monoclonal anti-FLAG M2 or anti-hexahistidine monoclonal antibody (Santa Cruz) at room temperature for 1 h and then with horseradish peroxidase-conjugated anti-mouse IgG antibody at room temperature for 1 h. The recombinant proteins were analyzed by SDS–12.5% PAGE under reducing conditions, stained with GelCord blue

stain reagent (Pierce), and detected by immunoblot analysis using anti-hexahistidine monoclonal antibody (Santa Cruz), anti-FLAG M2 monoclonal antibody, anti-human CD44 monoclonal antibody (clone 3C-11; Cell Signaling Technology, Inc., Beverly, MA), or anti-human TLR2 polyclonal antibody (clone TLR2.1; Santa Cruz). The stable knockdown clones (1×10^5 cells/well) were stimulated with FSL-1 (1 μg/ml), and degradation of IκBα and expression of CD44 and β-actin were determined by immunoblotting using antibodies specific to IκBα (Cell Signaling), CD44 (clone 3C-11), and β-actin (Sigma). The immune complexes and cell lysates were visualized with Super Signal West femto substrate (Pierce) and detected by using an LAS-3000 image analyzer system (Fujifilm, Tokyo, Japan).

DNA microarray analysis. Total RNA was extracted from Huh7 and HCV subgenomic replicon-harboring cells stimulated or not with FSL-1 (1 μg/ml) for 24 h by using an RNeasy minikit (Qiagen) and purified by using a QuickPrep mRNA purification kit (GE Healthcare Life Science, Little Chalfont, United Kingdom). Differentially expressed genes were screened with the use of a DNA microarray system, the human genome U133 plus 2.0 (Kurabo, Osaka, Japan). Data were analyzed by using the GeneChip operating software version 1.4 (Affymetrix 690036) with Microarray Suite version 5.0 (MAS 5.0). Differentially expressed genes were extracted using DNA microarray viewer (Kurabo), and then hierarchical clustering was performed by using Avadis 4.3 prophetic software (Strand Life Sciences, Bangalore, India).

Stable knockdown cell clones. The short interfering RNA (siRNA) sequences of the sense strands targeted to human CD44 (5′-GGAAAUG GUGCAUUUGGUGdTdT-3′), human TLR2 (5′-GCCUUGACCUGUC CAACAAdTdT-3′), and human MyD88 (5′-GGAGGAUUGCCAAAAG UAUdTdT-3′) were designed by using pSilencer Expression Vectors Insert Design Tool (Ambion, Austin, TX) and were introduced into the BamHI and HindIII sites of pSilencer 2.1 U6 Puro vector (Ambion). To establish stable knockdown cell clones, cells were transfected with the plasmids and drug-resistant clones were selected by treatment with puromycin (InvivoGen) at a final concentration of 1 μg/ml.

Real-time PCR. Total RNA was prepared from cells by using an RNeasy minikit (Qiagen), and the first-strand cDNA was synthesized by using a ReverTra Ace (TOYOBO, Osaka, Japan) and oligo$(dT)_{20}$ primer. Each cDNA was determined by using Platinum SYBR green quantitative PCR (qPCR) SuperMix UDG (Invitrogen) according to the manufacturer's protocol. Fluorescent signals were analyzed with an ABI PRISM 7000 (Applied Biosystems). The human IP-10, MIG, I-TAC, interleukin-8 (IL-8), HCV internal ribosome entry site (IRES), CD44, TLR1, TLR2, TLR4, TLR6, TLR7, TLR9, and glyceraldehyde-3-phosphate dehydrogenase (GAPDH) genes were amplified using the primer pairs 5′-GGCCATCAAGAATTTACTGAAAGCA-3′ and 5′-TCT GTGTGGTCCATCCTTGGAA-3′, 5′-TTAAATTCTGGCCACAGACAA CCTC-3′ and 5′-GCAGCCAAGTCGGTTAGTGGA-3′, 5′-CTTTCATG TTCAGCATTTCTACTCC-3′ and 5′-CCTATGCAAAGACAGCGTCCT C-3′, 5′-CCCAAGGACGGAGACTTCGAT-3′ and 5′-GAAACTTGCTG TGGGTGACCAT-3′, 5′-GAGTGTCGTGCAGCCTCCA-3′ and 5′-CAC TCGCAAGCACCCTATCA-3′, 5′-AACCCTTGCAACATTGCCTGA-3′ and 5′-GCTTCCAGAGTTACGCCCTTGA-3′, 5′-GGAGGCAATGCTG CTGTTCA-3′ and 5′-GCCCAATATGCCTTTGTTATCCTG-3′, 5′-GAA AGCTCCCAGCAGGAACATC-3′ and 5′-GAATGAAGTCCCGCTTAT GAAGACA-3′, 5′-AGGATGATGCCAGGATGATGTC-3′ and 5′-TCAG GTCCAGGTTCTTGGTTGAG-3′, 5′-CCTGGCAAGAGCATTGTGG A-3′ and 5′-TCGTAATGGCACTCACTCTG-3′, 5′-TCTTCAACCAGAC CTCTACATTCCA-3′ and 5′-GGAACATCCAGAGTGACATCACAG-3′, 5′-GGGACCTCGAGTGTGAAGCA-3′ and 5′-CTGGAGCTCACAG GGTAGGAA-3′, and 5′-ACCACAGTCCATGCCATCAC-3′ and 5′-TCC ACCACCCTGTTGCTGTA-3′, respectively. The expression of the mRNA of each gene was normalized to that of GAPDH.

Reporter assay. Cells seeded onto 12-well plates at a concentration of 1.5×10^5 cells/well were transfected with 100 ng of each of the plasmids encoding the luciferase gene under the control of the IP-10, endothelial-leukocyte adhesion molecule (ELAM), and IFN-stimulated response element (ISRE) promoters and stimulated with 500 μg/ml of HA or 250 ng/ml of IFN-α at 24 h posttransfection. Luciferase activity was determined with the dual-luciferase reporter assay system (Promega, Inc., Madison, WI) and the *Renilla* luciferase reporter gene was simultaneously transfected as an internal control.

Gene silencing by siRNA. siRNAs targeted to the endogenous human CD44 (5′-GGAAAUGGUGCAUUUGGUGdTdT-3′) and negative control no. 1, which exhibits no downregulation of any human genes, were purchased from Ambion. HCV replicon-harboring cells were transfected with 100 nM siRNA by using siFector (B-Bridge International, Sunnyvale, CA) according to the manufacturer's protocol.

Flow cytometry. The cell surface expression of CD44 and CD81 on Huh7 cells, cells harboring subgenomic replicons of JEV and HCV of genotypes 1b (Con1 strain) and 2a (JFH1 strain), and Huh7OK1 cells infected with HCVcc (JFH1) was analyzed by flow cytometry (Becton Dickinson, Mountain View, CA). Cells were washed twice in PBSF and incubated with mouse monoclonal antibodies to human CD44 (clone BU52; Ancell, Inc., Bayport, MN) and human CD81 (BD Biosciences). Mouse IgG1 and IgG2b (BD Biosciences) were used as isotype controls. Cells were washed with PBSF and incubated with the phycoerythrin (PE)-conjugated anti-mouse IgG monoclonal antibody.

Statistical analysis. Results were expressed as means ± standard deviations. The significance of differences in the means was determined by Student's *t* test.

RESULTS

Expression of IP-10 is specifically increased in cells replicating HCV upon stimulation with conventional TLR2 ligands. To examine the involvement of TLR signaling pathways in IP-10 production in cells replicating HCV, we determined the level of IP-10 mRNA in the HCV replicon-harboring and Huh7 cells upon stimulation with various TLR ligands. Among the TLR ligands we examined, PGN derived from bacterial components induced a significant enhancement of IP-10 production in the replicon-harboring cells but not in Huh7 cells (Fig. 1A). A dose-dependent induction of IP-10 was observed in the replicon-harboring cells treated with PGN (Fig. 1B). The enhancement of IP-10 production was also observed in the replicon-harboring cells in response to other TLR2 ligands, including FSL-1, Pam2CSK, and Pam3CSK, which are responsive to each of the heterodimers of TLR2/-6 and TLR1/-6, in contrast to the inhibition of IP-10 production in the replicon-harboring cells upon stimulation with poly(I·C) (Fig. 1C), which was probably due to interference in the dsRNA-dependent signaling pathway by NS3/-4A protease as described previously (25). The expression of TLR2 was confirmed not only in Huh7 and HCV replicon-harboring cells but also in primary human normal hepatocytes and human liver sinusoidal endothelial cells (Fig. 1D). To further examine the expression of each of the CXC chemokines in the HCV replicon-harboring cells, the level of mRNA of the CXC chemokines was determined by real-time PCR upon stimulation with PGN or IFN-γ. Although treatment with IFN-γ suppressed the replication of HCV and induced the expression of IP-10, MIG, and I-TAC in the replicon-harboring cells, stimulation with PGN induced the expression of IP-10 but not of MIG and I-TAC in the replicon-harboring cells (Fig. 1E).

We next examined the effect of HCV infection on the expression of CXC chemokines in cells upon stimulation with PGN. Huh7OK1 cells were established by the elimination of HCV RNA from the replicon-harboring cells by treatment with IFN (34). Huh7OK1 cells are highly permissive to HCVcc (JFH1 strain) in-

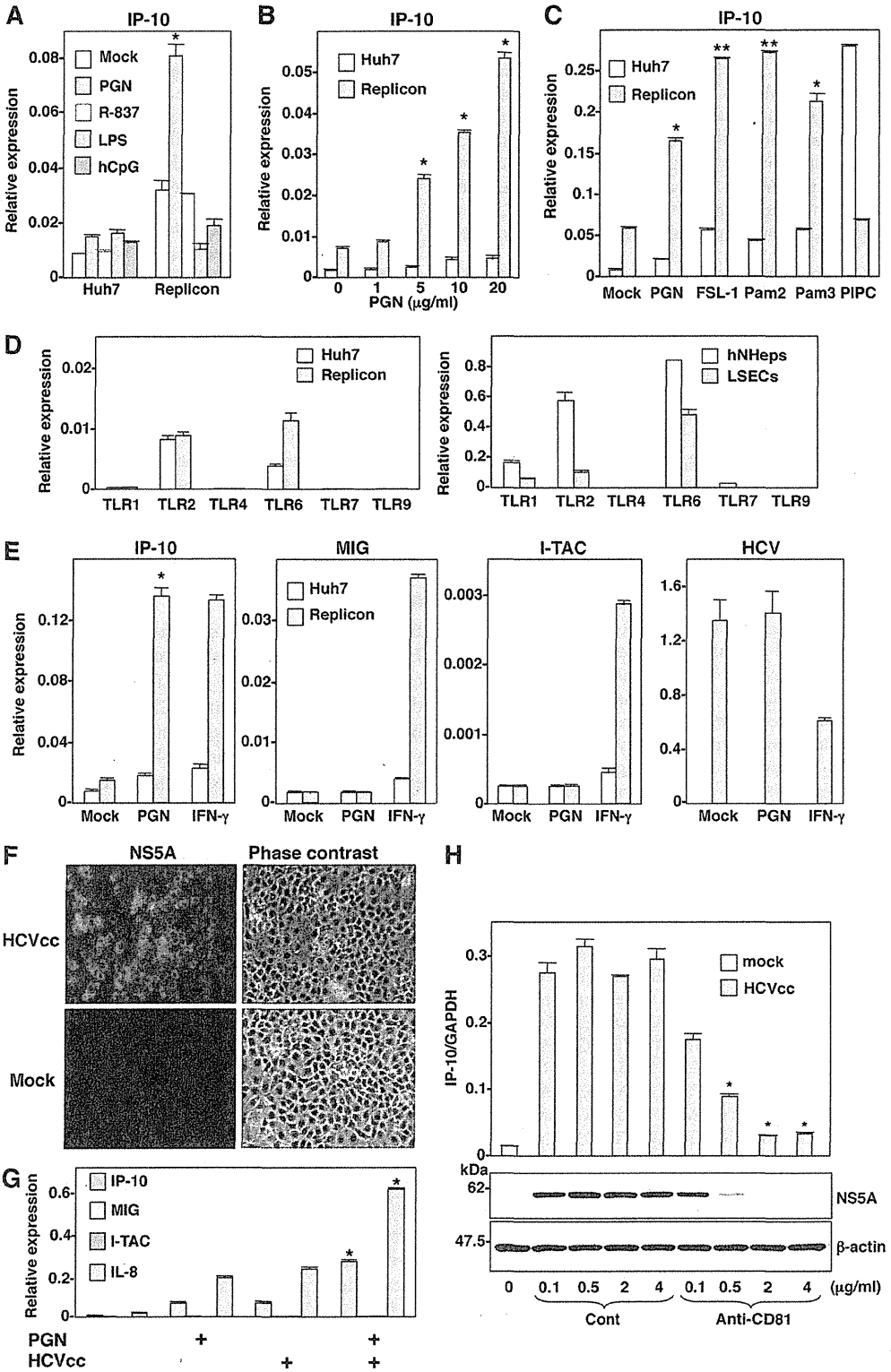

FIG 1 Enhancement of IP-10 production in the HCV-replicating cells upon stimulation with TLR2 ligands. (A) Huh7 and HCV replicon-harboring cells were stimulated with 20 μg/ml of PGN, 10 μg/ml of R-837, 20 μg/ml of LPS, or 10 μg/ml of hCpG, and the levels of IP-10 mRNA were determined by real-time PCR at 24 h after stimulation. (B) Huh7 and HCV replicon-harboring cells were stimulated with various concentrations of PGN, and the levels of IP-10 mRNA were determined at 24 h after stimulation. (C) Huh7 and HCV replicon-harboring cells were stimulated with 20 μg/ml of PGN, 1 μg/ml of FSL-1, 1 μg/ml of Pam2CSK (Pam2), 1 μg/ml of Pam3CSK (Pam3), or 50 μg/ml of poly(I·C) (PIPC), and the level of IP-10 mRNA was determined at 24 h after stimulation. (D) Total RNA was extracted from Huh7 cells, HCV replicon-harboring cells, primary human normal hepatocytes (hNHeps), and human liver sinusoidal endothelial cells (LSECs) cells, and expression levels of

fection, and most of the cells were infected within 7 days postinfection (Fig. 1F). Expression of IP-10 was induced in Huh7OK1 cells upon either stimulation with PGN or infection with HCVcc and was synergistically increased by costimulation (Fig. 1G). IL-8 is an inflammatory chemokine involved in HCV pathogenesis and a marker of the prognosis of CHC patients treated with IFN (37). In addition to IP-10, the production of IL-8 was also enhanced in Huh7OK1 cells infected with HCVcc upon stimulation with PGN (Fig. 1G). IP-10 production in Huh7OK1 cells upon infection with HCVcc was inhibited by pretreatment of cells with an anti-CD81 antibody in a dose-dependent manner in accord with the suppression of NS5A expression (Fig. 1H). These results indicate that the expression of IP-10 is specifically increased in cells replicating HCV upon stimulation with conventional TLR2 ligands.

Expression of CD44 is enhanced in cells replicating HCV and is associated with an increase of IP-10 production in response to TLR2 ligands. To determine the mechanism of enhancement of IP-10 production in cells replicating HCV upon stimulation with TLR2 ligands, the gene expression profiles in Huh7 and the replicon-harboring cells at 24 h after stimulation with a TLR2 ligand (FSL-1) were assessed by DNA microarray analysis. A variety of TLR2 ligand-inducible genes were regulated in the replicon-harboring cells upon FSL-1 stimulation (Fig. 2A). Among them, we focused on CD44 as a candidate molecule for participation in the enhancement of IP-10 production due to the significant enhancement of this molecule in the HCV replicon-harboring cells. CD44 is an adhesion molecule, a broadly distributed type I transmembrane glycoprotein, and a receptor for the glycosaminoglycan hyaluronan (HA). It has been shown that CD44 plays an important role in a variety of immunologic functions, including the adhesion, differentiation, homing, and activation of leukocytes and T cell extravasation to sites of inflammation (38). To confirm the data from the DNA microarray analysis, we examined the expression of CD44 in HCV replicon-harboring cells stimulated with TLR2 ligands. The expression of CD44 mRNA was upregulated in the replicon-harboring cells but not in Huh7 cells and was further enhanced by stimulation with FSL-1 or Pam3CSK in accord with the increase of IP-10 expression (Fig. 2B). Immunoblot analysis confirmed the enhancement of endogenous CD44 expression in the replicon-harboring cells (Fig. 2C). Furthermore, the cell surface expression of CD44 was also upregulated in the HCV replicon-harboring cells of genotypes 1b (Con1 strain) and 2a (JFH1 strain) but not in Huh7 and JEV subgenomic replicon-harboring cells (Fig. 2D), consistent with the enhancement of CD44 expression upon stimulation with FSL-1 (Fig. 2E). Furthermore, the expression of CD44 in the replicon-harboring cells was reduced by treatment with an HCV protease inhibitor (BILN2061), suggesting that enhancement of CD44 is dependent on the replication of HCV (Fig. 2F). These results suggest that the expression of CD44 is enhanced in HCV replicon-harboring cells autonomously replicating the HCV genome and is associated with an increase of IP-10 production in response to TLR2 ligands.

CD44 does not participate in the IP-10 production upon stimulation with TLR2 ligands derived from bacterial components. To further examine the involvement of CD44 in IP-10 production through the TLR2 signaling pathway, we assessed the effect of knockdown of CD44 expression on the IP-10 production in HCV replicon-harboring cells. Although transduction of small interfering RNA (siRNA) targeted to an ectodomain of CD44 which is well conserved among the CD44 variant isoforms suppressed the expression of CD44, IP-10 production upon stimulation with FSL-1 in the replicon-harboring cells exhibited no reduction (Fig. 3A). Similarly, the stable knockdown of CD44 in the HCV replicon-harboring cells did not show a reduction of IP-10 production upon stimulation with FSL-1 (Fig. 3B), suggesting that CD44 expression is not involved in IP-10 production upon stimulation with the conventional TLR2 ligands derived from bacterial components. Furthermore, the degradation of IκBα upon stimulation with FSL-1 was not affected by the stable knockdown of CD44 in the replicon-harboring cells (Fig. 3C). These results suggest that CD44 is not involved in the immune activation by stimulation with TLR2 ligands derived from bacterial components in cells replicating HCV RNA.

HA participates in IP-10 production in cells replicating HCV. Previously, it has been shown that a low-molecular-weight HA derived from the human umbilical cord acts as a TLR2 ligand in primary murine macrophage cells (41). Serum HA is derived from lymphocytes, fibroblasts, and hepatic stellate cells in the liver, and elevation of serum HA is an indicator for hepatic fibrosis and dysfunction of sinusoidal endothelial cells, because most HA is degraded in the hepatic sinusoidal endothelial cells (22). To determine the role of HA in IP-10 production in human hepatoma cell lines, we established Huh7OK1 cell lines stably expressing siRNA targeted to CD44, TLR2, or MyD88. The IP-10 production upon stimulation with HA was severely impaired by the knockdown of either gene (Fig. 4), suggesting that IP-10 production upon stimulation with HA is totally dependent upon the CD44-TLR2-MyD88 axis.

The production of IP-10 in the replicon-harboring cells was enhanced in both mRNA and protein levels by stimulation with HA (Fig. 5A). In addition to IP-10, the HCV replicon-harboring cells induced the expression of IL-8 but not of other CXCR3 ligands, including MIG and I-TAC, upon stimulation with HA (Fig. 5B). The enhancement of IP-10 production by stimulation with HA was also observed in the HCV replicon-harboring cells derived from other genotypes but not in the parental Huh7 cells and JEV replicon-harboring cells (Fig. 5C). The stable knockdown of CD44 in the HCV replicon-harboring cells significantly suppressed IP-10 production upon stimulation with HA but not with IFN-α and IFN-γ (Fig. 5D). The promoter region of IP-10 in-

TLR mRNA were determined by real-time PCR. (E) Huh7 and HCV replicon-harboring cells were stimulated with 20 μg/ml of PGN or 250 ng/ml of IFN-γ, and the IP-10, MIG, or I-TAC mRNA level and HCV IRES RNA level were determined by real-time PCR at 24 h after stimulation. (F) Huh7OK1 cells infected with HCVcc at a multiplicity of infection (MOI) of 1 and incubated for 7 days were fixed with 4% paraformaldehyde–PBS, permeabilized with 0.25% saponin, and immunostained with an anti-NS5A monoclonal antibody. (G) Huh7OK1 cells infected with HCVcc were stimulated with 20 μg/ml of PGN at 6 days postinfection, and the IP-10, MIG, I-TAC, or IL-8 mRNA level was determined by real-time PCR at 24 h after stimulation. (H) Huh7OK1 cells were treated with various amounts of antibodies against isotype control IgG (Cont) or human CD81 for 2 h at 37°C and infected with HCVcc at an MOI of 1. Levels of IP-10 mRNA and expression of NS5A were determined at 6 days postinfection by real-time PCR and immunoblotting, respectively. Data from real-time PCR were normalized to the amount of GAPDH mRNA. Asterisks indicate significant differences (*, $P < 0.05$; **, $P < 0.01$) versus the results for control cells or mock-infected cells.

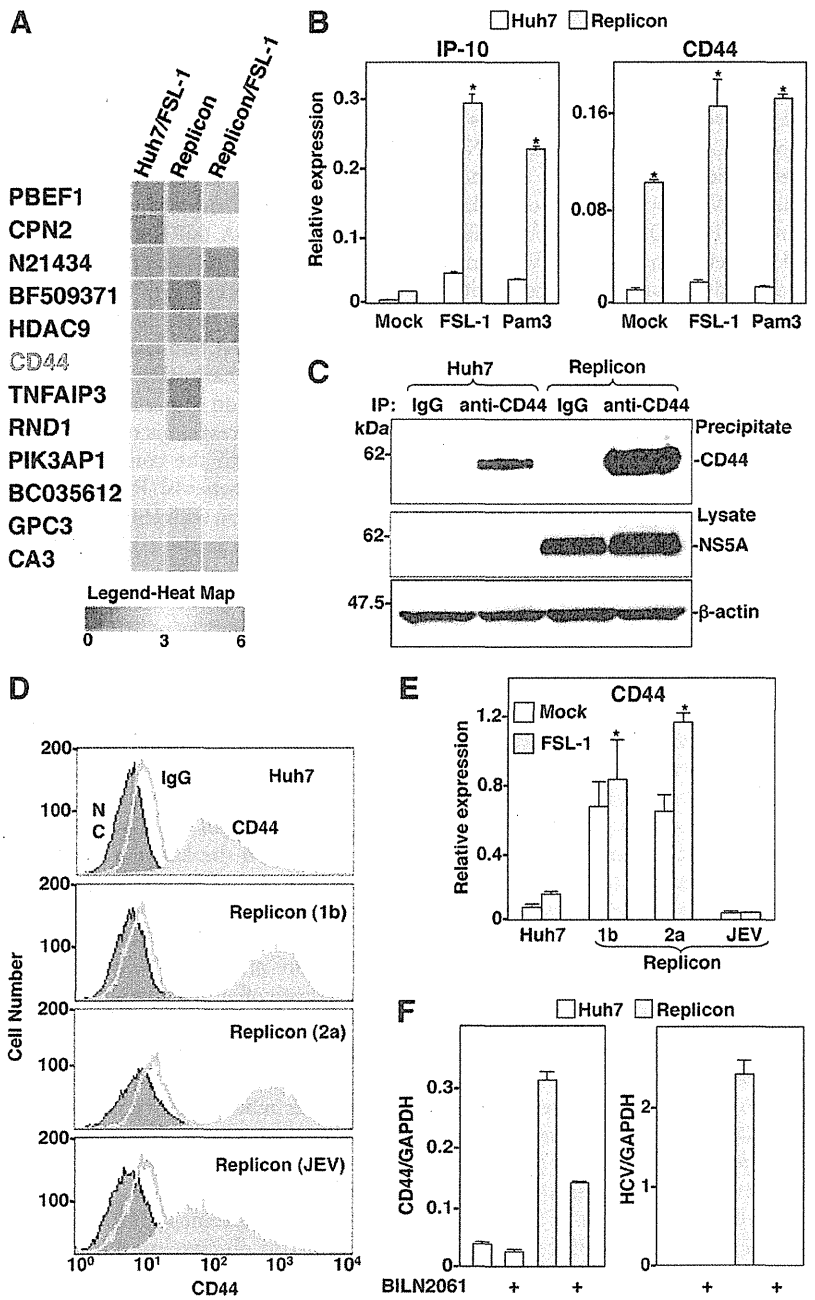

FIG 2 Expression of CD44 in HCV replicon-harboring cells is upregulated in accord with IP-10 production in response to TLR2 ligands. (A) Twelve genes in Huh7 and HCV replicon-harboring cells treated or not treated with FSL-1 were selected, and the resulting heat map is shown. PBEF1, pre-B-cell colony enhancing factor 1; CPN2, carboxypeptidase N, polypeptide 2; N21434, full-length insert cDNA YQ07B06; BF509371, unannotated protein; HDAC9, histone deacetylase 9; TNFAIP3, tumor necrosis factor, alpha-induced protein 3; RND1, Rho family GTPase 1; PIK3AP1, phosphoinositide-3-kinase adaptor protein 1; BC035612, *Homo sapiens* clone IMAGE:4183247 mRNA; GPC3, glypican 3; CA3, carbonic anhydrase III, muscle specific. (B) Huh7 and HCV replicon-harboring cells were stimulated with 1 μg/ml of FSL-1 or 1 μg/ml of Pam3CSK (Pam3), and the mRNA levels of IP-10 and CD44 were determined by real-time PCR at 24 h after stimulation. (C) Expression of CD44, NS5A, and β-actin in Huh7 and HCV replicon-harboring cells was determined by immunoblotting. IP, immunoprecipitation. (D) Cell surface expression of CD44 on Huh7 cells, HCV replicon-harboring cells derived from genotype 1b (Con1 strain) and 2a (JFH1 strain), and JEV replicon-harboring cells was determined by flow cytometry. The filled histograms of purple and orange indicate results for unstained (NC) and stained cells, respectively. Blue lines indicate results for isotype control. (E) Huh7 cells, HCV replicon-harboring cells (Con1 and JFH1 strains), and JEV replicon-harboring cells were stimulated with 1 μg/ml of FSL-1, and the level of CD44 mRNA was determined by real-time PCR at 24 h after stimulation. (F) Huh7 and HCV replicon-harboring cells were treated with 100 nM HCV protease inhibitor (BILN2061), and RNA levels of CD44 and HCV were determined at 72 h posttreatment. Data from real-time PCR were normalized to the amount of GAPDH mRNA. Asterisks indicate significant differences (*, $P < 0.05$) versus the results for control cells.